Engineering Geology of Alpine Tunnels: Past, Present and Future

S. Loew
Chair of Engineering Geology, Dept. of Earth Sciences, ETH Zuerich, Switzerland

G. Barla
Dept. of Structural and Geotechnical Engineering, Politecnico di Torino, Italy

M. Diederichs
Geological Engineering, Queen's University, Kingston, Ontario, Canada

ABSTRACT: This paper provides a review of engineering geological contributions to the design and construction of deep Alpine tunnels during the last 150 years. The progress and current status in engineering geological approaches and theoretical understanding of observed phenomena and geological hazards is discussed and documented with a large number of examples from traffic tunnels constructed in the European Alps. Major engineering geological, rock mechanical, and hydraulic lessons learnt from the recently completed Lötschberg and Gotthard Base Tunnels are highlighted. Hazards discussed in detail include strongly squeezing ground, spalling and rock bursting, and water inflows. The role of brittle fracturing and faulting in controlling these hazards is critically reviewed. State-of-the-art methods on how to cope with these hazards in design and construction are summarized. The paper is closing with an outlook into unresolved key issues that should be addressed in future interdisciplinary research and development initiatives.

1 INTRODUCTION

The Alps (Figure 2.1) form a part of a Tertiary orogenic belt of mountain chains, called the Alpide belt, that stretches through southern Europe and Asia from the Atlantic all the way to the Himalayas. The Alps formed essentially between the middle Cretaceous and Miocene as a result of the collision of the African and European tectonic plates, in which the western part of the Mesozoic Tethys Ocean, which was formerly in between these continents, disappeared. The Alps are composed of the pre-Triassic basement complex affected by Variscan and older orogenies, and Triassic to Oligocene sediments which were only deformed by Alpine movements. Permo-Carboniferous sediments occupy an intermediate position.

The Alps are subvided into the Western, Central and Eastern Alps. In the northern part of the Central Alps (Figures 2.2), basement and cover show quite different tectonic behavior; in most places the cover rocks have been stripped away from their basement, to form décollement nappes. In the southern part of the Central Alps, Alpine deformation and medium to high grade metamorphism have largely obliterated the original differences of competence and structure. The Alps are bounded in the north and south by large and flat molasse basins, filled with several kilometer thick Tertiary debris from Alps. The 3-dimensional tectonic structure of the Alps is very complex and heterogeneous due to small-scale breakup of Pangäa in Cretaceous time, creating a variety of micro-continents and basins, and the subsequent oblique thrusting during and after subduction of the Tethys ocean.

Today the European Alps form a major water divide with mountains rising up to 4800 meters height and a width of about 150 to 200 kilometers (Figure 2.1). In the Western and Central Alps there are several places, where there is only one ridge or pass to cross, to which access is gained by a deep-cut valley. The passes which cross a single ridge, and do not involve too great a detour through a long valley of approach, became the most important and the most popular routes for travel and transportation, e.g. the Mont Cenis, the Great St. Bernard, the St. Gotthard, the Septimer and the Brenner. These passes first became known to the outside world when the Romans crossed them to raid or conquer the region beyond. A few passes (e.g. the Semmering, the Brenner, the Col de Tende and the Arlberg) had carriage roads constructed before 1800, while those over the Umbrail and the Great St. Bernard were not completed till the early years of the 20th century. Most of the carriage roads across the great alpine passes were thus constructed in the first half of the 19th century, largely due to the Napoleon's need for such roads as modes of military transport.

Alpine tunnels helped to cross the Alps also in winter time and became major technical achievements in engineering geology and civil engineering in the second half of the 19th century and the 20th

century. In recent years new types of transalpine tunnels have been constructed or designed. These transalpine base tunnels cross the Alps without ramps at the elevation of the molasses basins north and south of the Alps, and are engineered constructions of dimensions never seen before.

This paper summarizes some of the engineering geological achievements and failures of historical tunnel constructions in the Alps (Chapter 2), reviews the current state-of-the-art in engineering geologic and geotechnical contributions to deep Alpine tunneling (Chapter 3) and finishes with an outlook into critical unresolved issues of deep tunneling (Chapter 4).

2 HISTORY OF TRANSALPINE TUNNEL CONSTRUCTIONS

2.1 *Tunnels constructed in the 19th and 20th century*

First traffic tunnels through the European Alps (Frejus Railway, Gotthard Railway, Lötschberg, Simplon, Arlberg) were constructed as part of transalpine railway lines in the second half of the 19th century and the beginning of the 20th century (Figure 2.2). The length of these tunnels ranged between 10 and 20 kilometers with maximum overburden of 700 to 2100 meters. All tunnels constructed during this period were designed as straight lines between the portals. Tunnels were excavated with pilot tunnels from both portals, and with a small gradient for free water drainage, requiring careful topographic surveys. The portals were located such that tunnel length and overburden were minimized but at the same time maintaining safe railway operation in winter time on the access ramps.

The first Alpine tunnel was the Frejus Railway Tunnel (Mont Cenis Tunnel) which, proposed in 1838, was finally started in 1857. It took 13 years to excavate a 12 kilometer length through calcschists. It was during the excavation of the Frejus that air drills and water power to drive air compressors started to be used instead of hand drilling with an increase of the rate progress by five times. The Frejus was followed by the excavation of the Gotthard Railway tunnel between 1872 and 1882, when better drilling machines became available and were mounted upon rail carriages, six or eight drills at a time (Harding 1981).

The most important engineering geological contributions to the design of these tunnels were predictive longitudinal geological sections. As deep rotary drilling technologies were not available at that time, geological surface mapping and drilling of pilot tunnels were the most important methods for the geological predictions of deep tunnels. On the other hand the second half of the 19th century was the period when major concepts of Alpine tectonics - such as nappe tectonics - were developed. Therefore some tunnel projects, like the Simplon Base Tunnel, were confronted with strongly differing geological predictions and public debates lasting several decades.

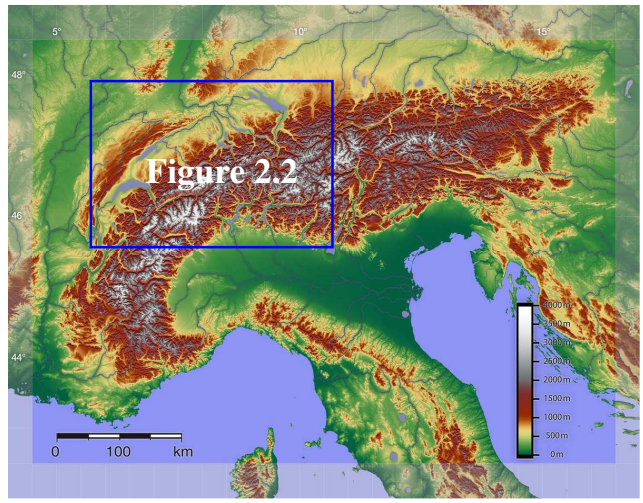

Figure 2.1. Topography of the Alps.

The biggest geologically driven catastrophe occurring in this period was the collapse of the Lötschberg Railway Tunnel on 23rd July 1908 (Figure 2.3 & 2.5). The chief engineer Dr. F. Rothpletz wrote in the unpublished memoirs: "On this day the working face of the bottom heading pilot tunnel reached a distance of 2.65 km from the start of the tunnel at Kandersteg… The rock, which was permeated with calcite veins, was a very compact black alpine limestone… The bottom of the Gastere Valley and the Kander river were situated 172 m above the pilot tunnel… At 3 a.m. I was awoken by an engineer and went into the deserted tunnel to find out what had happened. 1200 m from the portal we came across a pile of rubble. It was soon apparent that at a distance of about 1500 m from the portal the tunnel was filled with debris, out of which some water flowed… The whole crew (25 miners) was lost. Investigations in the Gastere Valley revealed a funnel-shaped collapse of about 80 m diameter and 3 m depth – that is: breakthrough of the rock face due to blasting of the last attack… and inrush of loose material from the Gastere Valley sediments into the tunnel… The assumption of the geological report, that there was still 100 m of firm limestone rock above the tunnel must be wrong."

The wrong interpretation of the bedrock elevation was based on rock outcrops at high elevation at the outlet of the Gastere Valley, and the assumption of a bedrock depth following the classical longitudinal profile of all rivers (a smooth concave-upward curve from the outlet of the valley to the headwater near the glaciated summits). The Gastere Valley shows

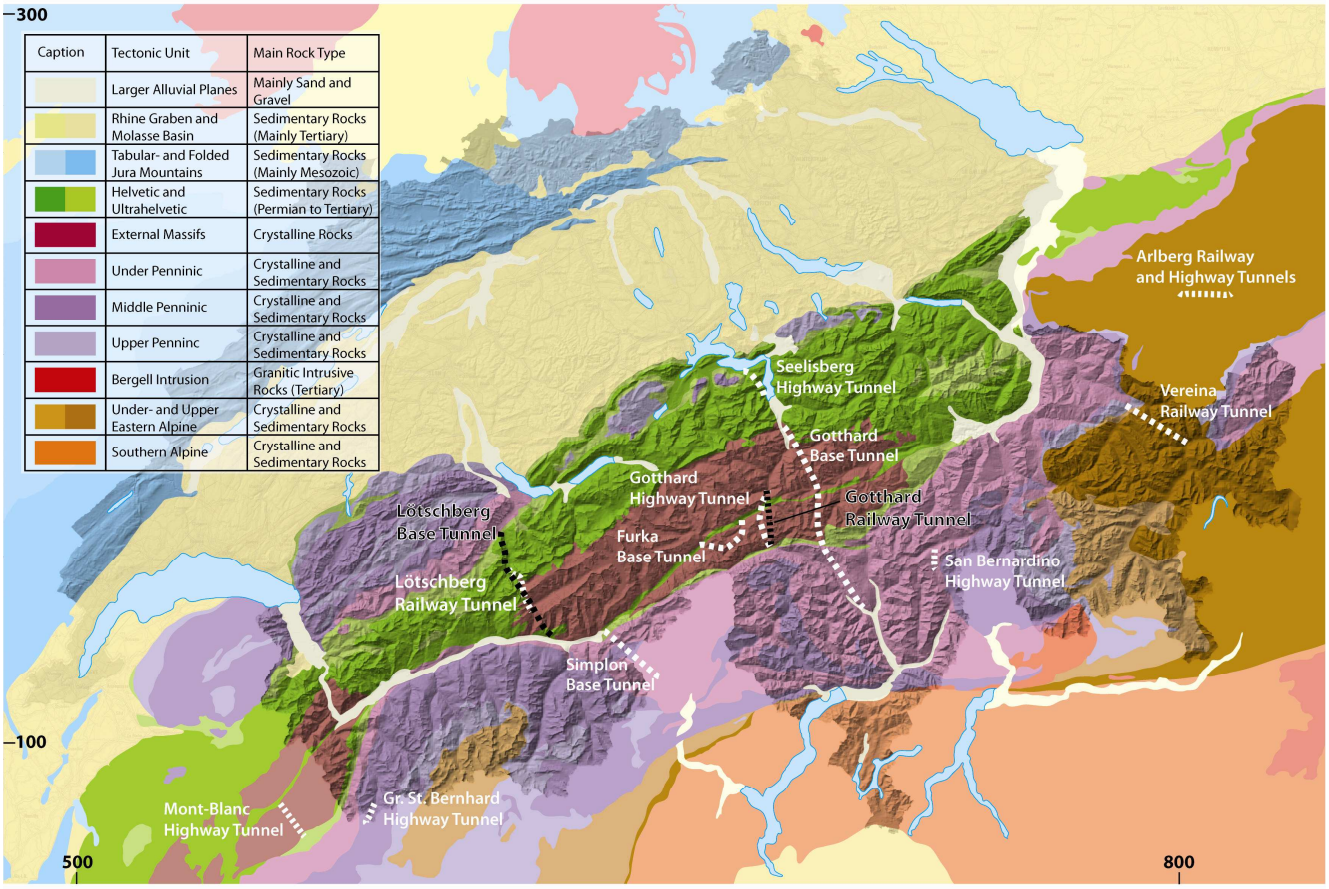

Figure 2.2. Tectonic map of the Central Alps, showing the location of major Alpine tunnels. Numbers refer to the Swiss kilometer grid.

the classical U-shaped morphology of glacial erosion, but it was not known at that time, that glacial erosion can carve deep basins without surface runoff into the basement rocks. Two shafts that were sunk into the infill of the Gastere Valley after the catastrophy showed that the trough was filled with glacial till, fluvial sediments and scree. After discussing various stabilization methods (such as freezing and grouting) it was decided to avoid the entire glacial trough by by-passing in the bedrock at the bottom of the Gastere Valley.

In the 19th century the engineering geological documentation of the encountered conditions was often done with great care and lead to important descriptions of many types of geological hazards we are confronted with today in deep tunneling. However, interpretations of high water inflows, strongly squeezing ground and rock bursts were incomplete or misleading as theoretical knowledge of rock stress, rock mass properties and groundwater hydraulics were very limited.

In the second half of the 20th century the increase in road traffic lead to a period of intensive road tunnel constructions through the Alps (Great St. Bernard, Mont Blanc, Gotthard Highway Tunnel, Frejus Road Tunnel). In contrast to the century before, engineering geological tunnel design could be based on a reliable description of Alpine geology, supported by local information from deep drillings. In addition, some knowledge about rock stress, rock mass behavior and deep groundwater flow was considered in the evaluation and selection of the tunnel routes, which therefore deviated from straight lines. Nevertheless unexpected ground behavior sometimes led to severe delays and cost overruns. Most of these unexpected adverse geological conditions were related to brittle faults, squeezing ground, rock bursting, sugar grained rocks, and deep seated slope deformations. In addition environmental impacts such as the drying out of springs through tunnel drainage became an important issue.

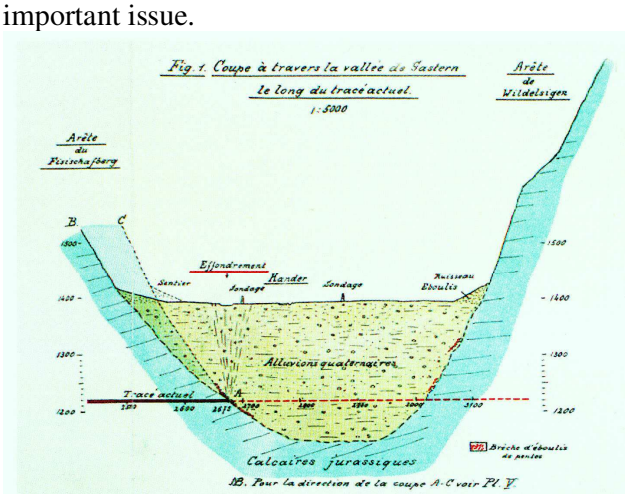

Figure 2.3. Simplified longitudinal section through the Gastere Valley. From unpublished Report (1909).

The 11.6 km long Mont Blanc Tunnel, between Courmayeur (Italy) and Chamonix (France), started in 1957 and took seven years to complete. The maximum overburden in granite under the l'Aguille du Midi is 2480 m, where sudden rock bursting phenomena were reported to occur. The Mont Blanc tunnel saw some of the first attempts to use the overcoring methods for the determination of the in situ state of stress in a side drift, 22.5 m far from the tunnel axis, under a cover of 1350 m (Oberti et al. 1969). Even at great depth this tunnel was confronted with large inflows from faults.

The 16.9 km long Gotthard Highway Tunnel has its portals at the same locations like the Gotthard Railway Tunnel, but follows the river bed of the Gotthard Reuss river in a curved alignment (Figure 2.6). The extra length of tunnel was accepted in favor of shorter ventilation shafts, reduced overburden, and greater vertical distance to deep soil infillings in the glacial trough of Andermatt. The Gotthard Highway Tunnel was confronted with strongly squeezing ground in tectonized Mesozoic sediments and crystalline bedrock. High initial inflows from brittle faults at great depth caused large scale consolidation settlements, which were observed for the first time in hard crystalline bedrock (Zangerl et al. 2006, 2008a, 2008b).

The 12.9 km long Frejus Road Tunnel, which links the city of Modane in France to the city of Bardonecchia in Italy, was excavated a few years later and opened in 1980. Aligned for a significant length nearly parallel to the old Frejus Railway Tunnel, it crosses almost entirely the calcschist formation. The overburden along a significant tunnel length is over 1000 m with a maximum of 1800 m. Significant rock mechanics studies were undertaken in this tunnel both in the laboratory and in situ. Of relevance is the back analysis of the mode of deformation with typical squeezing phenomena. It was demonstrated that the convergences are to be analyzed by taking into account the immediate convergence due to the advance of the face and the time dependent convergence due to the rheological behavior of the rock mass (Panet 1996).

2.2 *Ongoing and recent tunnel constructions*

The Alpine tunnels constructed today are important components of high-speed transalpine railway corridors (Figure 2.4). They cross the mountain belt at the elevation of the main cities and basins located to the north/west and south/east of the Alps and are therefore longer (up to 57 kilometers) and deeper (up to 2500 meters) than all tunnels constructed in the centuries before. Of particular importance are the recently completed 34 km long Lötschberg Base Tunnel and the 57 km Gotthard Base Tunnel which will have its main cut-through in fall 2010. The predictions and anticipated engineering geological problems of the Gotthard and Lötschberg Base Tunnels are described in (Loew et al. 2000). Other tunnelling projecs in the Alps include the 57 km long base tunnel along the Lyon-Turin rail line and the Brenner Base Tunnel, which is planned to be 55 km long.

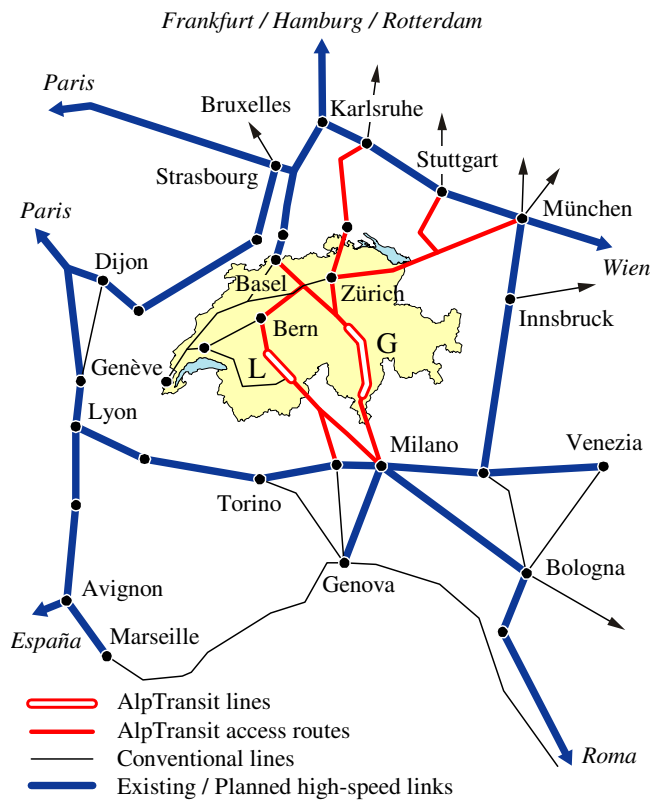

Figure 2.4. AlpTransit Base Tunnels and high-speed railway links in the Alps (L: Lötschberg Base Tunnel, G: Gotthard and Ceneri Base Tunnel). Other base tunnels discussed in this paper link Torino with Lyon (Lyon-Turin base Tunnel) and Innsbruck with Milano-Venezia (Brenner Base Tunnel).

The majority of the applied engineering geological methods used to design these tunnels are descriptive and very similar to the road tunnels constructed in the second half of the 20th century. The main differences are related to the exploration methods, which today also regularly include surface and borehole based geophysical investigations and in some cases the use of directional drilling. However, many geophysical methods applied during the preliminary investigations or subsequently during construction have not always met their goals in complex alpine tectonic settings. Our current understanding of the major geologic hazards, as described in Chapter 3, is illustrated with many examples from the recently constructed base tunnels. Therefore a short summary of these tunnels is given below.

2.2.1 *Lötschberg Base Tunnel*

The Lötschberg Base Tunnel (LBT) is 34.6 kilometers long, single-track single-tube railway tunnel crossing the northern part of the Swiss Alps at an el-

evation between 655 m.a.s.l (Portal Raron) and 828 m.a.s.l. (apex). The tunnel was constructed with 3 intermediate adits (lateral ramps of Steg, Ferden and Mitholz). The highest overburden is about 2000 m.

Preliminary investigations started in 1990 and included 27 deep exploration boreholes, the construction of a 9.6 km long exploration/service tunnel (called Kander Valley) from the northern portal at Frutigen, the construction of a 700 m long exploration tunnel from the southern portal at Raron, and geological projections from existing near-by underground traffic and hydropower excavations in the southern section. The selection of the tunnel alignment focused on avoiding major geological hazards, and was carried out in an iterative process, starting from about 50 options in 1990. For the final tunnel alignment high priority was given to avoiding deep glacial troughs, and minimizing tunnel sections in karstic limestones, evaporitic sediments, graphitic schists, and major fault zones. The construction of the lateral adits started in 1997 and of the main tunnel bores in 1999. The tunnel excavations were completed in April 2005 and the tunnel went in commercial operation mid-2007.

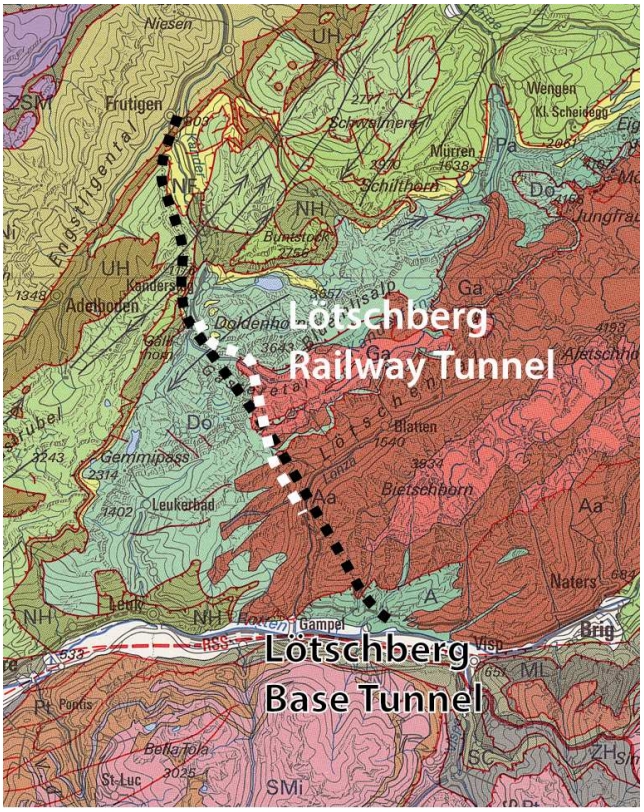

Figure 2.5. Tectonic map with the final alignment of the Lötschberg Base and Railway Tunnel. NF: Flysch, NH: Wildhorn Nappe, Do: Doldenhorn Nappe and autochthonous sediments north, Aa: Aar Massif, A: autochthonous sediments south. Geology from swisstopo (2005).

A geological section at the scale of 1:50'000 has been published by Ziegler (2006). The tunnel crosses from north to south (Figure 2.5) the Taveyannaz sandstones, Paleogene flysch, tectonic mélange, 4 slices of the Helvetic Wildhorn Nappe (primarily flat laying limestones and schists), and a large recumbent fold with units of the Helvetic Gellihorn and Doldenhorn Nappe (Paleogene flysch and limestones/marls). Below and south of the Doldenhorn Nappe the tunnel crosses over a short distance autochthonous Triassic and Jurassic sediments and enters finally into the crystalline basement of the Aar Massif composed of granitic plutons of Variscan age embedded in older gneisses, schists, phyllites and amphibolites. Inside the crystalline basement a new 650 m wide trough filled with Jurassic and Permo-Carboniferous sediments was encountered close to the Northern margin in addition to three thin Triassic and Jurassic sediment slices, and one already known Carboniferous slice at Ferden. At the southern portal autochthonous sediments (limestones, marls, schists and sandstones) are folded and thrusted into the bedrock of the Aar Massif. Two deep fluvio-glacial basins occur above the base tunnel and are filled with thick Quaternary infillings (Kander Valley, Gastere Valley). Brittle faults occur with high frequencies in several orientations and styles, the two widest ones are the phyllitic fault zones of Dornbach and Faldumbach.

For design and construction purposes the final tunnel alignment has been subdivided into lithostratigraphic sections. Due to the comprehensiveness of the preliminary investigations, the reliability of the geological and hydrogeological prediction, as described in the tender documents from December 1998, was generally very good. The only major geological difference was the new Permo-Carboniferous trough with strongly squeezing ground located in the northern Aar massif. Here convergences reached up to 0.9 m, mainly in intensively deformed phyllites and up to 1m thick anthracite layers. Generally the occurence of brittle spalling and rock bursting in the Aar Massif (with overburden between 1200 and 2000 meter) was not as intense as expected. But spalling and bursting in front of the TBM cutter head created excavation problems. Sometimes rock bursts in the face were so violent, that after the ejection of blocks the TBM cutter head vibrated for some minutes.

The total steady state tunnel inflow rate as measured in 2005 amounts to about 80 l/s at the South Portal. The total outflow at the North Portal amounts to 150 l/s. While all the tunnel sections in the Flysch, the Tectonic Mélange, the Wildhorn Nappe and the crystalline basement did not yield substantial amounts of groundwater, biggest long term water inflows occur in the fractured and karstified limestones of the Doldenhorn Nappe (120 l/s as of 2006). The second biggest long term inflows are related to karstified carbonaceous sedimentary rocks of the southern autochthonous sediment cover. Finally, inside the crystalline body of the Aar Massif the two

thin mesozoic sediment slices with carbonate rocks which initial generated cumulative discharges to all open exploration boreholes of about 45-50 l/s, had to be grouted in order not to impact the thermal springs of Leukerbad. After a successful grouting operation these tunnel inflows reduced to about 2.5-3 l/s.

The highest tunnel inflow rates in the Doldenhorn Nappe occured in karstified limestones. However, as discussed in Pesendorfer and Loew (2009) and Pesendorfer et al. (2009) the karst pipes encountered at the elevation of the Base Tunnel are old sediment-filled (i.e. completely clogged) paleokarst structures, which formed when the base level of the receiving stream in the Kander valley was deeper than the local elevation of the LBT. Today, the paleokarst of the LBT is essentially decoupled from the active near surface karst system, which is controlled by the actual elevation of the Kander river. Therefore the flows into the LBT are mainly controlled by brittle fault systems and show very stable long term inflow rates, typical for fractured rock at greater depth. This behavior is substantially different for the active shallow karst systems in the autochthonous sediments south, and the inflows to the old Lötschberg railway tunnel, which show strong annual discharge variations.

The most significant impacts on surface springs were recorded close to the tunnel portal in the south. Here tunnel drainage of karstified Lias limestones below the village of St. German resulted in a significant groundwater pressure drop within 2 months (from 18 to 1 bar at the tunnel elevation) and the drying out of 3 important karst springs. Drainage of karst springs at the village of St. Germain also drained the overlying Quaternary sediments. These are composed of 70 m thick rock fall deposits with layers of peat and sand/silt with high contents of organic matter (Vuilleumier & Seingre 2002). These sensitive layers strongly reacted to the groundwater drainage which led to surface settlements of up to 180 mm in 4 months.

2.2.2 *Gotthard Base Tunnel*

As the longest tunnel of the AlpTransit corridor in central Switzerland, the Gotthard Base Tunnel is 57 kilometer in length and connects Erstfeld in northern Switzerland to Bodio in southern Switzerland (Figure 2.6). The highest overburden is 2500 m. The Gotthard Base Tunnel has been built using 3 intermediate adits (Amsteg, Sedrun, Faido) and was therefore divided into 5 working lots. While two of these adits are lateral ramps of up to 4 km in length, the central point of attack of the Gotthard Base Tunnel consists of two vertical shafts of 800 m depth. The construction work of the adits started in 1996 and of the primary tunnel sections in 2000. Tunnel excavation will be completed in fall 2010.

Preliminary investigations started in 1986 and included 6 deep exploration boreholes near Sedrun, the construction of a 5 km long exploration tunnel (Piora Tunnel) from Faido, complete geological mapping (1:10'000) above the tunnel route, rock mass characterizations, and a detailed fault inventory. The selection of the tunnel alignment focused on crossing the Piora zone (in surface outcrops and a shallow hydropower drift: karstified dolostones and limestones, cornieules and sugar grained dolomites) over the shortest possible length and reducing the overburden. The tunnel alignment was no changed much compared to initial proposal, made already in 1963 (Scheider 1999).

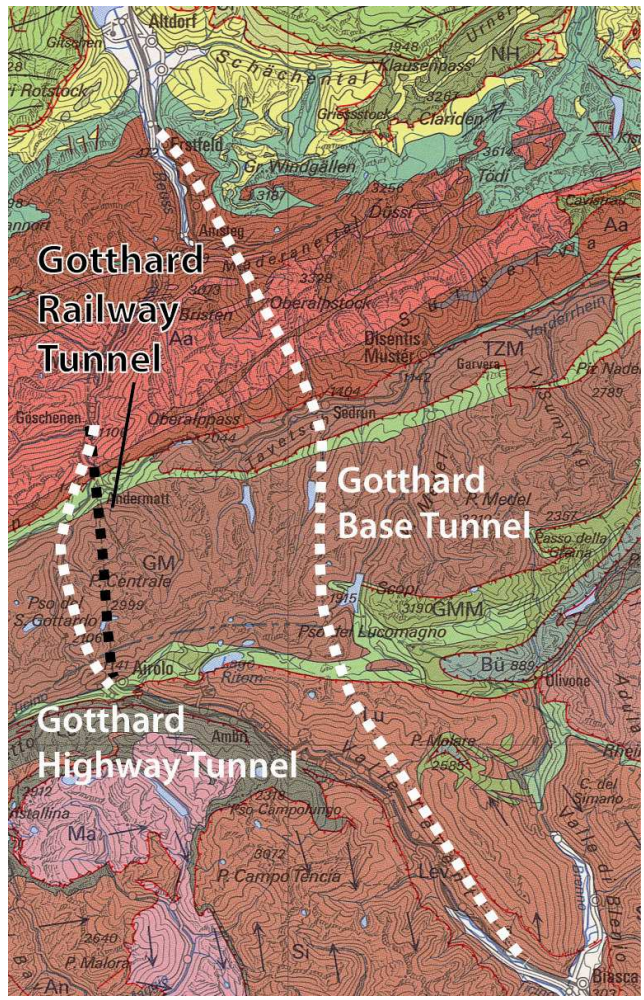

Figure 2.6: Tectonic map with the final alignment of the Gotthard Base Tunnel, Gotthard Highway and Gotthard Railway Tunnel. Aa: Aar Massif, TZM: Tavetsch Massif, GM: Gotthard Massif, GMM: Mesozoic cover of GM, including Piora Zone, Lu: Lucomagno Nappe, Lev: Leventina Nappe. Geology from swisstopo (2005).

Figure 2.6 shows the geological conditions along the Gotthard Base Tunnel. Starting in the north, the tunnel passes through 8.5 km of the Aar Massif, which shows similar rocks and structures as those intersected by the southern Lötschberg Base Tunnel: Pre-Variscan basement with Variscan plutonic and volcanic rocks, Pre-Alpine foliation overprinted by a steep Alpine schistosity and ductile to brittle faults of only a few meters thickness running nearly nor-

mal to the tunnel axes. To the south follows the Tavetsch Massif which is separated from the Aar Massif by two faults of 40 m thickness each with a high content of fault gouge. The northernmost 1000 m of the Tavetsch Massif incorporates strongly sheared schists intersected by a dense cataclastic fault pattern. The southern part of the Tavetsch Massif, with a thickness of about 2000 m, shows substantially different and much better tunneling conditions. Here intact Pre-Variscan gneisses, schists, pegmatites and pyroclastic rocks can be found, intersected by narrow cataclastic fault zones (less than 5% of total length).

More to the south, the Gotthard Base Tunnel intersects the 460m thick Urseren Garvera Zone, composed of Permo-Carboniferous phyllites and schists, and Triassic to Jurassic schists, greywackes, cornieules, quarzites limestones and dolomites. The Gotthard Massif follows to the south, covering a length of 12.4 km, and is composed of similar rock types like that of the Aar Massif: late Variscan granitic intrusions (the Medelser and Cristallina granodiorite) and older polymetamorphic basement rocks intersected by steeply dipping brittle and brittle-ductile faults. The (par-)autochthonous sediments to the south of the Gotthard Massif are referred to as Piora Zone. At tunnel elevation the rocks in this zone differ substantially from the near-surface lithologies, and include a strong, coarse grained and layered anhydrite-dolomite-sequence of 125 m length and 10 m of strongly sheared gneisses and schists (Fellner 1999, Herwegh & Pfiffner 1999).

The Penninic Gneiss Zone to the south of the Piora Zone can be subdivided into the steeply inclined and folded Lucomagno Nappe (mafic and granitic gneisses) and the flat laying Leventina Nappe (granitic gneisses). These rocks are again transected by a great number of flat and steeply inclined ductile and brittle fault zones (generally a few meters in thickness or less).

The geological prediction of the Gotthard Base Tunnel was generally very good; the only major differences were related to boundaries of Variscan granitic intrusions, not seen at ground surface (Frei & Breitenmoser, 2006). In tectonized rocks of the northern Tavetsch Massif and brittle faults ground behavior was as expected. However, groundwater inflows from faults and fractures occurred at other locations, than where they had been expected. This is mainly due to the fact, that the architecture and hydraulic properties of faults and fracture sets can not be predicted over depths of more than 1 kilometer. In addition, the unexpected location and orientation of brittle faults in the Penninic Gneiss Zone created large stability problems, both in TBM excavations of the main bores and drill and blast excavations of the Faido multifunction station (Röthlisberger, 2006; Bonzanigo & Oppizzi, 2006).

2.2.3 *Brenner Base Tunnel*

The Brenner Base Tunnel is the main infrastructure to be built along the railway corridor between Munich (Germany) and Verona (Italy), a section of the North-South axis of the European high speed rail link (Figure 2.4). The final design consists of two tunnels, 55 kilometers long, with a centre tunnel used during construction as a guide tunnel used to determine geological conditions, and later for drainage and emergency access. There will be cross over between the tunnels every 333m. Each main tube has a circular cross section with 4 m radius. The maximum overburden is expected to be 1600 m, with a mean value of 900 m approximately.

In the summer of 2006 work started on a first pilot tunnel excavated by a double-shield TBM through the Brixen granite complex between Aica and Mules (Italy). The second one will be excavated between Ahrental and Innsbruck (Austria).

The geology in the project area is characterized by Mesozoic continental units of European and Adriatic/African origin and also by oceanic units, which are piled into nappes, due to Alpine orogenesis. The most commonly encountered rocks are phyllites, schists, gneiss and granite. Brittle deformations including three large fault systems are expected to occur along the tunnel alignment.

2.2.4 *Lyon-Turin Base Tunnel*

The Lyon-Turin Base Tunnel is to be excavated with minimal slope between the two portals in Italy and France. Nearly 57 kilometers in length, this tunnel will comprise two parallel tubes with a circular cross section of 4 m radius. The maximum overburden is 2500 m and more than 10 kilometers length will be excavated under 2000 m of overburden.

At present one access adit (Saint Martin La Porte) is being excavated and two adits (La Praz and Modane) are complete. These adits will provide multiple excavation faces for construction and will subsequently be used for ventilation and to allow access for maintenance and rescue teams if necessary. They are essential for understanding the geological, hydrogeological, and geomechanical conditions along the tunnel and for the selection of the excavation method to be used for the Base Tunnel.

In the Lyon-Turin Base Tunnel the Alpine chain is crossed from West to East, perpendicular to the large alpine units such of the Subbrianconnaise, the Brianconnaise, and the Piedmont zone. Significant problems under discussion at this time are posed by the crossing of the Carboniferous Formation, where severe to very severe squeezing problems are expected to occur. Also of relevance is the excavation through the Ambin Massif, with gneiss and micaschists, where both spalling and rock bursting phenomena will be encountered.

3 CURRENT UNDERSTANDING OF GEOLOGICAL HAZARDS IN ALPINE TUNNELLING

The major geological hazards as encountered in recently constructed Alpine tunnels relate to the prediction and behavior of faults at depth, water inflow in heterogeneous fractured or karstified rock masses, stress-induced tensile failure of hard rocks, and plastic shear failure and squeezing of weak rocks (mainly fractured schists, phyllites and cataclastic fault rocks). In this chapter current understanding of these hazards is presented in detail with the main focus on 1) experiences made in recent base tunnel constructions, and 2) engineering geological predictions for future Alpine tunneling projects.

3.1 *Brittle Faults and Structurally Controlled Failures*

3.1.1 *Hazards and Fault Types*

Faults can cause a diversity of hazards in deep Alpine tunneling, ranging from high water inflows (Section 3.4) to strongly squeezing ground (Section 3.2), to rock bursting (Section 3.3) and structurally controlled failures (e.g. Deere 1973; Keller & Schneider 1982; Schubert 1993, 2006; Schubert & Riedmüller 1997).

Structurally controlled failures are mainly controlled by reactivations of the pre-existing fracture network and not by the formation of new discontinuities. They can vary in dimension, from falls or breakouts of individual blocks to the collapse of the tunnel face and crown over the typical length of a tunnel diameter (Figure 3.1). In this section we will only discuss large scale structurally controlled, i.e. fault controlled, failures. Small scale block failures are a regular but minor issue in deep tunneling, mainly controlled by a proper support installed in the crown immediately behind the TBM shield or after each round in a drill and blast tunnel, which is important for worker safety. A support package could include a systematic bolting pattern or a mesh to retain individual blocks, firmly and frequently anchored by bolt plates, straps and/or arch segments.

Figure 3.1. Face collapse in steeply dipping fault (Gotthard Base Tunnel, chainage 5353 East Tube, September 10, 2009).

The impact of faults on underground excavations depends on fault type, fault architecture, fault dimension, fault orientation, excavation type and temporary support measures. Faults intersecting a tunnel at right angle (Figure 3.1) cause much less difficulty in underground excavations than faults that are near parallel to or cross the tunnel axis at a low angle (Figure 3.2).

Brittle faults as defined in the geological literature belong to shear zones, which are narrow zones of highly strained rock characterized by spatial gradients of finite strain. The amount of strain is generally highest within the centre of the shear zone, decreasing outward into the wall rocks adjacent to the zone. Another characteristic feature is their anastomosing geometry, encompassing and wrapping around more rigid, less deformed rock bodies (i.e. shear lenses or knockers). Four general types of shear zones can be defined based on the dominating type of deformation (e.g. Ramsay & Huber, 1987; Davis & Reynolds, 1996; Sibson 1977):

1. Ductile shear zones display structures that have a metamorphic aspect and record shearing by ductile flow. The deformation processes within ductile shear zones are mainly achieved by crystal plasticity and thus involve only a minor amount of fracturing. In the structural geology literature these hard, fine-grained metamorphic rocks are often referred to as mylonites (e.g. Passchier & Trouw, 1996). This is contrary to the term mylonite used in the sense of the greek word μύλος *mylos*, implying mechanical abrasion of grains by milling.

Figure 3.2. Roof collapse above TBM shield in flat lying fault (Gotthard Base Tunnel, Bodio Section).

2. Brittle shear zones, generally termed faults or fault zones (a series of closely spaced faults), contain fractures and other features formed by brittle deformation mechanisms (mainly cataclasis). Displacement occurs along a network of closely spaced fractures. Based on primary cohesion cataclastic fault rocks can be classified into cohesionless (fault breccias, fault gouge) and cohesive (cataclasite). Due to the high permeability of the fractured material, hydrothermal inflow is promoted and faulting is often accompanied by hydrothermal activity, and crystal growth leading to cementation and sealing. Cohesionless clay rich fault rock in outcrop is often called kakirite.
3. Semi-brittle shear zones include en-échelon veins or joints and stylolites and involve mechanisms such as cataclastic flow and pressure solution.
4. Brittle-ductile shear zones show evidence of both brittle and ductile deformation.

In this paper only brittle faults, brittle fault zones, and brittle-ductile shear zones are discussed, because ductile and semi-brittle shear zones do not generate instability problems in underground constructions.

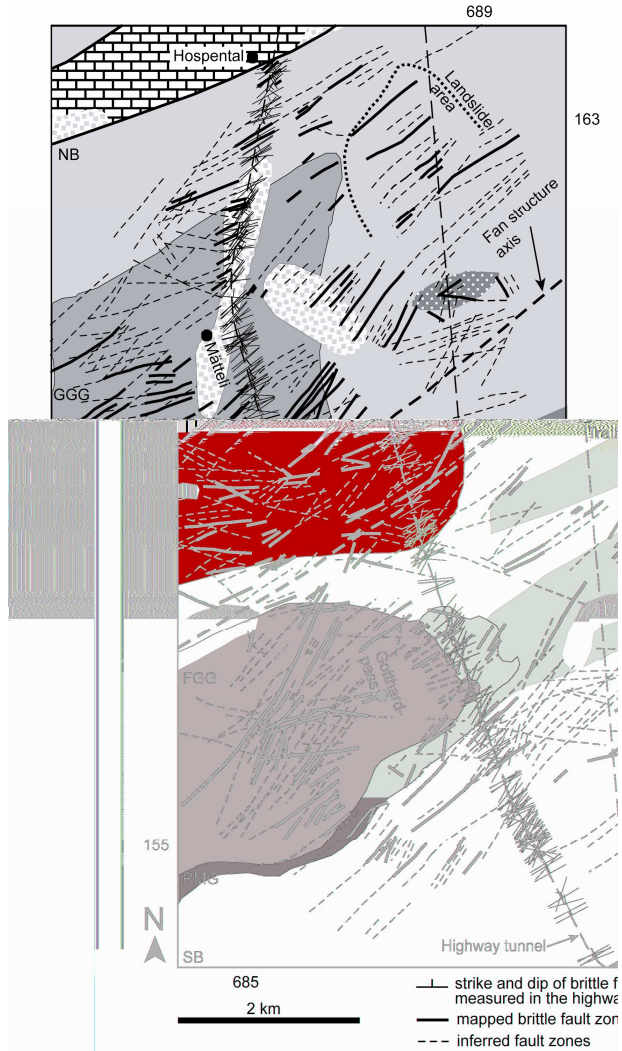

Figure 3.3. Brittle faults mapped in the Gotthard pass area above the Gotthard highway and motorway tunnels. Black lines represent fault rocks mapped in the field, dashed lines represent inferred faults from aerial photos and geomorphological mapping. From Zangerl et al. 2006.

3.1.2 *Prediction of brittle faults*

The prediction of brittle faults mainly relies on morphological mapping in the field and on high-resolution digital terrain models. For steeply dipping faults in Alpine areas, these approaches are reliable, as long as the mapped lineaments are verified with structural geologic observations (Figures 3.3 & 3.4) and are not covered with soil deposits (glacial tills or colluvium).

Faults with shallow dip angles (< 30º) often do not show clear morphological expressions and are underestimated or overseen in mapping campaigns. A dramatic example of this kind is the low angle brittle fault encountered at the Bodio section of the Gotthard Base Tunnel (Figure 3.2; Bonzanigo & Oppizzi 2006). Here, a nearly flat laying cataclastic zone with impermeable gouge layers of up to one meter thickness, undulating around gneiss lenses with dip angles between 20º and 60º, followed both TBM tunnel tubes over more than 500 meters.

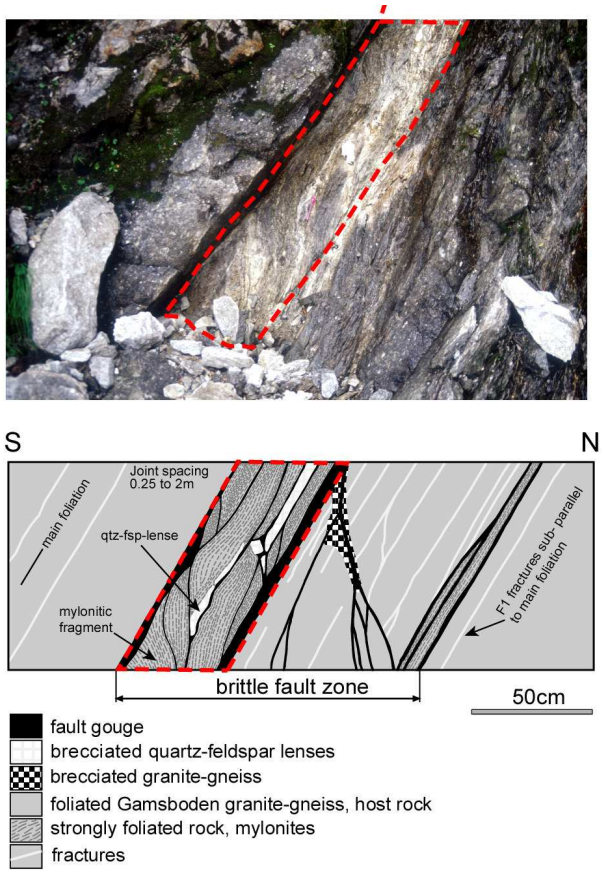

Figure 3.4. Photo and front view of the internal composition of a brittle-ductile fault. From Zangerl et al. 2006.

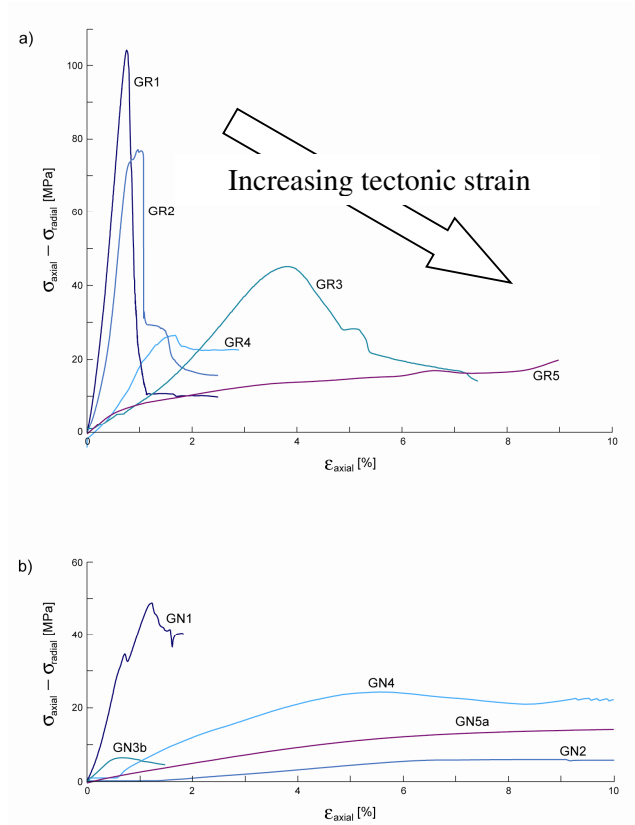

Figure 3.5. Stress-strain curves for fault rocks in granite (a) and gneiss (b). Increasing brittle tectonic overprint (e.g. fracture density) changes sample response from brittle (GR1, GR2, GN1) to ductile (GR5, GN2, GN5). From Laws et al. 2003.

Individual faults have a diverse internal architecture, composed of fault rocks with strongly variable mechanical and hydraulic properties (Wallace & Morris, 1996; Chester & Logan 1996). Some faults show a symmetric composition, with a central zone of highly strained, fine grained, low permeability fault rocks (the fault core), bounded by a damage zone with an increased fracture density and permeability in comparison to the intact protolith. Figure 3.4 shows an example of small brittle-ductile fault, composed of fault gouge, brecciated gneiss, foliated and mylonitic gneiss, and a damage zone with increased density of persistent fractures. In granitic rocks Laws et al. (2003) showed that, with increasing degree of brittle tectonic overprint, sample strength decreases and rock behavior shows a transition from brittle to ductile deformation (Figure 3.5). These trends may be explained by increasing fracture densities, increasing foliation intensity, increasing thickness of fine-grained, low cohesion fracture infill, and increasing mica content associated with the increasing degree of tectonic overprint. Faults occur on all scales, but their frequency-size (in terms of widths and lengths) relation follows a power-law distribution, i.e. large faults are rare compared to small faults.

In tunneling, large difficulties are normally related to fault zones at project relevant scales, i.e. a series of spatially overlapping or mechanically interrelated faults. The stability problems are not only a result of the fault rock weakness, but also of the mechanical and hydraulic heterogeneity of fault rocks at these scales. The heterogeneous nature of brittle fault zones not only leads to heterogeneous distributions of displacements, but also to stress concentrations in the more competent blocks. As summarized in Schubert (2006) different modes of failures can be observed. While in sections dominated by gouge, the typical post peak behaviour will be rather ductile, the more competent blocks may fail in a brittle manner.

3.1.3 *Instabilities associated with brittle faults*

Ductile faults can create regions of increased squeezing. Recognition of these zones is essential for proper ground management. As seen in Figure 3.6, a yielding support system can be utilized in the vicinity of the fault similar to that discussed later for squeezing ground. In this example the fault created excessive squeezing requiring re-mining. The support was effective however in controlling deformations and allowing continuous operations in spite of the displacement.

Figure 3.6. Squeezing ground in a fault zone with yielding support systems. Photo courtesy of E. Hoek.

Brittle faults are a major problem in mining environments or in larger excavations in tunnel projects such as stations and cross-over caverns. They normally pose less of a problem to the actual tunnels themselves. There are exceptions however. Faults that are near parallel to or cross the tunnel axis at a low angle are problematic for wall stability. Moreover, the faults can connect long lengths of tunnel wall, releasing large amounts of energy upon failure. An example is shown in Figure 3.7. In this example, a steeply dipping fault is crossed by the tunnel at a small oblique angle. As the tunnel heading nears the point of intersection between the tunnel axis and the fault, the fault becomes progressively closer to the tunnel wall. In hard ground this causes a channelling of stress into the pillar of rock between the wall and the fault. As the fault nears, the failure mode will change from spalling (A) to strain bursting (B) to fault slip rupturing the tunnel boundary (C). In a worst case, the wall rock will not yield under the increased loading until the tunnel intersects the fault. In this case, the release of the fault at the heading will cause a chain reaction back along the fault and cause instantaneous failure at A, B and C, resulting in a large energy release and significant damage or extreme risk of injury or fatality.

There is no clear strategy to counter this hazard. In a drill and blast tunnel, restricted entry protocols (long production delays after each blast) can improve worker safety, allowing for bursting to occur without worker exposure. In TBM drives, this phenomenon remains a significant challenge.

Faults that cross the tunnel at a high angle (near-perpendicular) can also pose a significant hazard for face bursting. As the tunnel approaches the fault, stress channelling can cause yielding in the face. In hard rocks this manifests as violent face spalling or face bursting (full face failure) near the fault. An example is shown in Figure 3.8. If the fault has displaced the lithology to bring a softer unit ahead of the fault, the difference in stiffness between the tunnel host rock (stiff) and the rock behind the fault (soft) will increase the risk of face overstress and bursting. The risk of face bursting can be reduced through pre-conditioning. In this method, 4 to 8 long blast holes are drilled out from the face near the perimeter of the tunnel and at a minimum lookout angle. These holes are blasted with the heading round or during a TBM stoppage. The effect is to create random fracturing in the rock mass so that the face yields in a more ductile fashion.

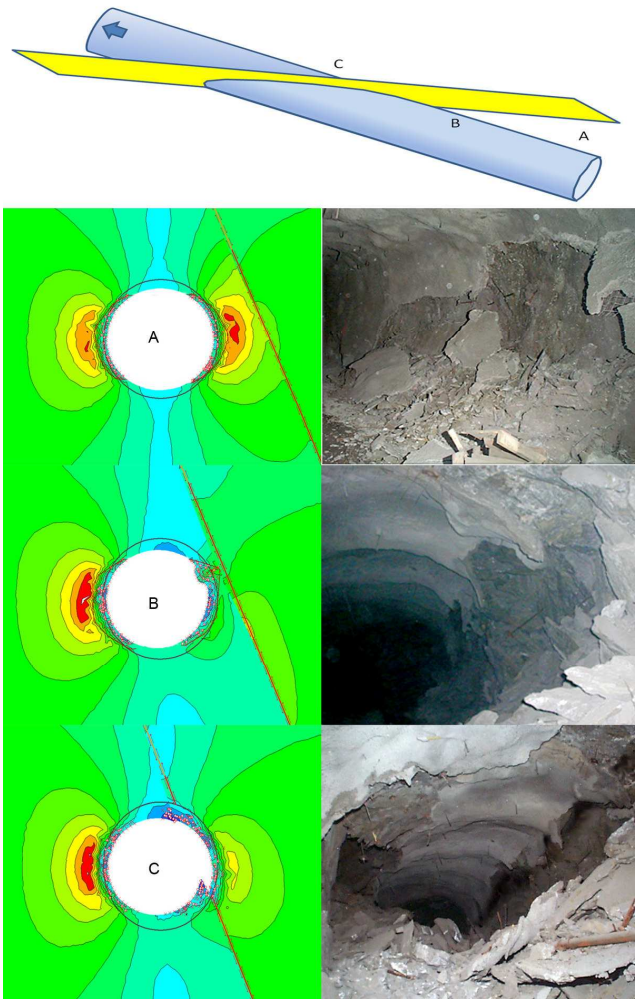

Figure 3.7. A tunnel approaching and intersecting a fault. Wall failure is initially in the form of spalling (A), strain bursting (B) and tunnel wall offset by fault (C).

Low cohesive brittle faults can result in sections of structurally controlled instability of several metres width along a tunnel. Additionally, wider zones of brittle deformation or fracturing in the presence of fluids can generate wide zones of vein networks or fracture-fill. These zones can then become decoupled from the regional stress field and result in low confinement block instability.

Alternatively, foliation or parallel fracture fabric generated in the vicinity of a fault can result in localized buckling instability (in the face or along the tunnel wall if the fault zone is subparallel to the tun-

nel axis. For horizontal faults, this fabric creates beam instability in the roof.

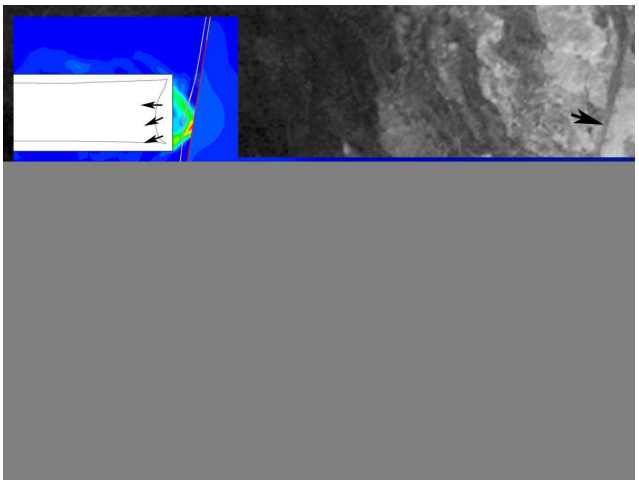

Figure 3.8. Faceburst caused by tunnelling into a brittle fault (arrow in photo). Inset shows increased shear strain (yielding) as face interacts with slipping fault.

Figure 3.9 illustrates several examples of structurally controlled failure encountered as tunnels pass through fault zones. In the first case (a), the fault zone manifests as a zone of intense parallel foliation. This results in highly anisotropic failure (buckling) in the sidewalls of a small pilot tunnel. The example in b) shows the retention (through a combination of grouted and anchored bolts and heavy mesh) of blocky rubble created in a fault zone within otherwise massive gneiss. The example in c) shows a mining tunnel at 2000m depth with full collapse resulting from total loss of confinement within a zone of faulted metasediment.

In each case, the key to success in these zones is correct anticipation of the fault zones as the tunnel advances and a timely increase in both reinforcement (grouted bolts) and holding elements (strong anchored bolts and heavy mesh or mesh over steel sets). The key to success in these cases lies in the ability to maintain a uniform tunnel profile (circle or arch). If the tunnel shape is lost through minor caving then the ability to control the stability as a whole is diminished.

Figure 3.9. Examples of structurally controlled instability in fault zones: a) strong foliation or parallel fractures in a fault zone parallel to the tunnel; b) progressive block destabilization in a TBM drive through a brittle fault zone; c) complete collapse and loss of confinement within a highly fractured fault zone at 2000m depth.

3.2 *Squeezing Ground*

3.2.1 *Hazards and Influencing Factors*

Squeezing is associated with a reduction of the tunnel cross section which is being excavated and with large time dependent deformations ahead of the face and in the rock surround, as shown typically in Fig-

ure 3.10 in the case of Saint Martin La Porte, an access adit to the Lyon-Turin Base Tunnel currently under construction. In general, in such conditions excavation may be carried out successfully by conventional methods even when very severe to extreme squeezing conditions are encountered. However, it is matter of debate in Alpine tunneling today if one may in such conditions use tunnel boring machines (TBMs).

Figure 3.10. Saint Martin La Porte access adit (Lyon-Turin Base Tunnel). Deformed horse-shoe section compared with the new yielding cross section implemented following re-profiling. From Barla (2009).

3.2.2 *Squeezing prediction*

The prediction of squeezing conditions along the tunnel alignment in long deep tunnels as the Alpine base tunnels is associated with a high level of uncertainty. This is due to the difficulties in defining the geological and hydrogeological conditions in general and to the fact that squeezing is not only associated with typical weak rock formations (such as phyllites, schists, serpentinites, claystones, shales, etc.), but it is also found to occur in highly fractured and heterogeneous rock masses.

Additionally, squeezing is dependent on a number of factors such as the in situ state of stress and the stress ratio (i.e. the minimum in situ principal stress divided by the corresponding maximum principal stress), and the pore water pressure in the ground. It is found to occur in contact and tectonized zones and faults; it is enhanced by the unfavorable orientation of discontinuities, such as bedding planes and schistosities. Therefore, the occurrence of such conditions in deep tunnels is difficult if not impossible to be predicted.

Empirical and semi-empirical approaches have been developed and are available in the rock mechanics literature (Barla 2001) to predict squeezing. The empirical approaches are based on case studies and define squeezing in terms of the overburden depth H and the Q rock mass classification index (Barton et al. 1974; Singh et al. 1992; Goel et al. 1995). The semi-empirical approaches provide tools for estimating the expected deformation around the tunnel and/or the support pressure required, by using analytical/numerical solutions for a circular tunnel in a hydrostatic stress field (Aydan et al. 1993). The common starting point of all these approaches is the use of the "competency factor", i.e. the ratio of uniaxial compressive strength σ_{ci}/σ_{cm} of intact rock/rock mass to overburden stress $p_o=\gamma H$ (γ= rock mass unit weight).

The most frequently used approach of this type is due to Hoek (2001) who, in the 2000 Terzaghi lecture on "*Big tunnels in bad rock*", by means of axisymmetric finite element analyses and a range of different rock masses, in situ stresses and support pressures p_i gave the following approximate relationship for tunnel strain ε_t (defined as the percentage ratio of radial tunnel displacement to tunnel radius):

$$\varepsilon_t(\%) = 0.15(1 - p_i / p_o)\frac{\sigma_{cm}}{p_o}^{-(3p_i/p_o+1)/(3.8p_i/p_o+0.54)}$$

A diagrammatic representation of this equation for zero support pressure (p_i) which may be used as a tool for a first estimate of tunnel squeezing problems is shown in Figure 3.11.

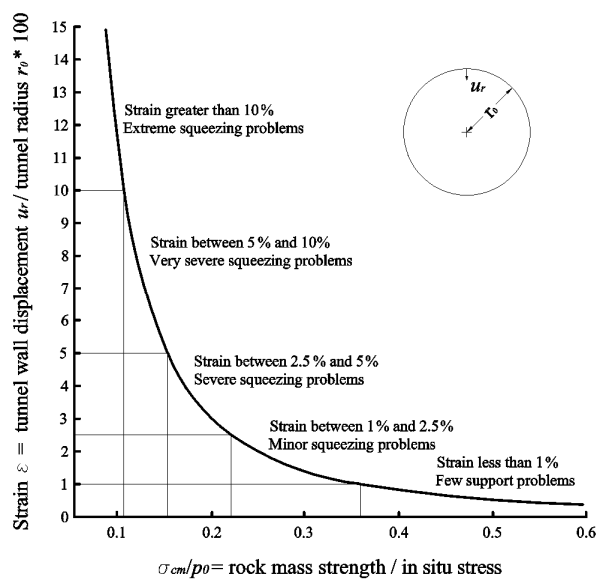

Figure 3.11. Squeezing problems associated with different levels of tunnel strain. From Hoek (2001)

Most often squeezing is found to occur in highly heterogeneous ground under anisotropic in situ stress, which is highly problematic to describe in any detail before tunnel excavation takes place. Figure 3.12 illustrates typical tunnel scale geological zones, characterized by highly heterogeneous, disrupted and fractured conditions of the rock mass, which exhibited very severe squeezing problems during the recent excavation of the Saint Martin La Porte ac-

cess adit in the Carboniferous Formation comprising black schists, sandstones, coal, clay-like shales and cataclastic rocks.

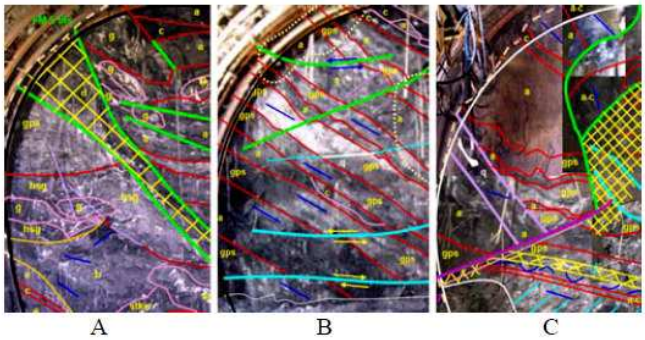

Figure 3.12. Tunnel face maps showing typical tunnel scale geological complexities in squeezing ground: A) Faulted; B) Laminated; C) Chaotic. Saint Martin La Porte access adit of Lyon-Turin Base Tunnel. From Branscombe et al. (2010)

In such cases, the geological conditions lead to severe to very severe convergences during excavation as shown in Figure 3.13, along array 1-5, between chainage 1250 and 1600 m approximately, with the face being 15 m and 30 m ahead of the monitoring section. Here it was found that the severity of squeezing is dependent on the percentage of coal, clay-like shales and cataclastic rock (the "weak components") with respect to schists and sandstones (the "strong components"). Also important in the onset and development of large deformations around the tunnel is the orientation of faults and laminations (Figure 3.12): it was found that in general, squeezing is enhanced significantly if these geological features strike parallel to the tunnel axis.

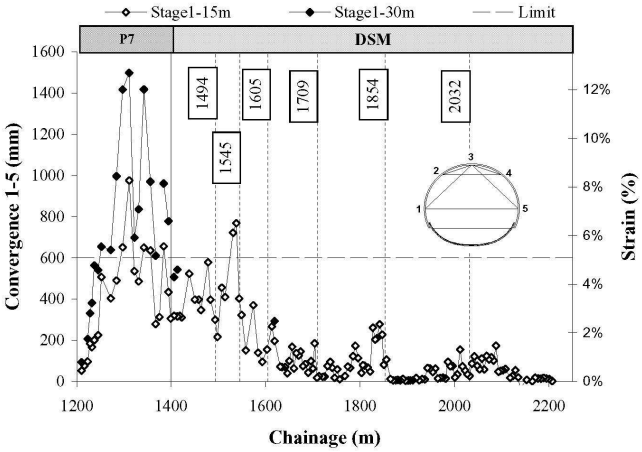

Figure 3.13. Saint Martin La Porte access adit. Convergences measured 15 and 30 m behind the face, between chainage 1200 and 2100 m approximately. From Barla (2009).

Similarly, during the excavation of the Lötschberg Base Tunnel in the Mitholz South section, the unexpected Permo-Carboniferous trough with weak sedimentary rocks (graphitic marls, sandstones and siltstone, containing alternating beds of anthracite coal up to 1 m thick, Figure 3.14) lead to very severe squeezing problems. Some tunnel sections in anthracite (coal) bearing Carboniferous sediments lead to convergences of up to 100 cm, 100 days after excavation (Sandrone et al. 2006). A critical zone with extreme squeezing conditions, about 1150 m long, was also encountered in the Gotthard Base tunnel, while excavating through the Northern Tavetsch Massif. Here, alternating layers of intact and variable strength cataclastic gneisses, slates, and phyllites were encountered in a very large fault zone (Cantieni & Anagnostou 2007). Squeezing conditions are also anticipated in some lengths of the Brenner Base Tunnel.

Figure 3.14. Tunnel face map showing complex geological conditions in anthracite (coal) bearing Carboniferous sediments. Lötschberg Base Tunnel, Permo-Carboniferous trough.

With the above in mind it is easily understood that the potential to predict tunnel squeezing problems at an early design stage in deep tunnels is rather limited. One may argue that if a good geological model can be developed, one should be able to optimize the tunnel route in order to avoid the problems of excavating in difficult geological zones where squeezing conditions might occur. However, it is to be recognized that most often the alignment constraints might be such as to make it impossible to avoid such zones, independent of the level of understanding of the geological conditions one may have achieved.

At present, with the experience gained in Alpine tunneling so far, the most reliable prediction of the squeezing problems to be encountered along base tunnels can be effected through the excavation of pilot or exploration tunnels, where excavation procedures and sequences, stabilization measures ahead and behind the tunnel face can be tested effectively for possible ranges of parameters, and controlled by an interactive observational method which implies the systematic use of geological and geomechanical

mapping during face advance, performance monitoring and back analysis. Known sections with squeezing ground can also be characterized successfully with directional core drillings from ground surface (Tavetsch Massif Gotthard Base Tunnel).

3.2.3 *Stiff versus yielding support systems*

Of the available options for conventional tunnel excavation and construction in squeezing rock (e.g. multiple headings, top heading and benching down, full face), the most recent method used is the full-face method (Figure 3.15). Here, a significant advantage is the large working space available at the face, so that large equipment can be used for installing support/stabilization measures at the tunnel perimeter and ahead of the face (Figure 3.15). However, this method requires a systematic reinforcement of the face and of the ground ahead. One of the two methods, "heavy" and "light", can be applied (Kovari 1998).

With the "heavy method" ("resistance principle"), the primary lining is designed to be very stiff (generally composed of steel fibre shotcrete and heavy steel sets) and the "ring is closed quickly" (Figure 3.15). The final concrete invert (first) and final concrete lining (second) are cast within a short distance from the face. It is apparent that if very high rock pressures are expected, as is the case of deep Alpine tunnels, this solution soon becomes impractical and one is to use the "light method" ("yielding principle"), where large deformations are allowed to develop around the tunnel with the expectation that rock pressure will decrease with increasing deformation. The excavation profile in such a case is chosen so as to maintain the desired clearance and to avoid re-profiling. A key point is to be able to control the development of deformations. A suitable tunnel support system is to be adopted that will allow for accommodating deformations without damage of the lining.

A yielding support system, which has been originally applied in mines and is still used today, consists of providing sliding joints in top hat steel sets (TH, Toussaint-Heintzmann type) embedded in the shotcrete lining. The tangential force in the steel sets is controlled by the number and by the pre-tensioning level of the sliding joints in the steel sets. Open gaps are provided with dense rock bolting of the tunnel cross section. After a pre-defined amount of convergence these gaps are filled with shotcrete.

Various design options have been proposed for tunnel applications to better deal with severe to very severe squeezing conditions such as the Lining Stress Controller - LSC element (Schubert 1996; Schubert et al. 1999); the WABE honey-comb element (Geomechanics & Tunnelling 2009); the highly Deformable Concrete element (Kovari 2005). This latter element is to be considered has the most innovative technological development when tunneling in squeezing rock conditions.

Figure 3.15. Full face excavation and construction method: face reinforcement (top) and ring closure (bottom).

TH steel sets were used in both the Gotthard and the Lötschberg Base Tunnels (Figure 3.16). In the latter case, following some local instabilities taken place in one of the cross passages between the two tubes, the decision was to change the cross section to circular and to add LSC elements in longitudinal cuts (Sandrone et al. 2006). Highly Deformable Concrete elements were instead used systematically along a significant tunnel length (500 m) of the al-

ready mentioned Saint Martin La Porte access adit of the Lyon-Turin Base Tunnel (Barla 2009).

Figure 3.16. Yielding support system with sliding joints in top hat steel sets embedded in the shotcrete lining as applied in the Gotthard Base Tunnel.

As shown in Figure 3.17, which illustrates this tunnel in its most severe squeezing conditions encountered (Figure 3.13, DSM cross section, chainage 1440-1600 m), a total of 9 such elements (height 40 cm, length 80 cm, and thickness 20 cm) were placed in slots in the shotcrete lining between the TH type steel stets installed with 1 m spacing. The installation of this yielding support system allows controlled deformations to take place. The elements have been designed to yield at 40-50 %, strain with a yield stress of 8.5 MPa. This means that with 9 elements installed, if one takes for simplicity a circular tunnel, under the assumption that each element may attain a 50 % strain, the maximum allowed radial displacement is equal to 20 cm approximately, resulting in a total tunnel convergence of 40 cm. Also, if one takes a yield stress σ_θ of 8.5 MPa, the radial confinement stress on the surrounding rock results to be 0.3 MPa approximately (Barla 2009).

3.2.4 *Assessment of rock mass behavior*

The rock mass behavior in squeezing conditions is characterized by a time-dependent response of the tunnel, slow movements of the same cross section during standstill, a large extent of the zone of influence of the excavation, and a long lasting tendency to undergo deformations. In cases, as already noted, the rock mass is highly heterogeneous with anisotropic behaviour. The complexity of the problem and the difficulties to account for time dependent deformations lead at the design stage to the adoption of simplified models of behaviour where the rock mass is assumed to follow an elasto-plastic ideally plastic model, with strength and deformability properties estimated in "short" and "long term" conditions.

Figure 3.17. Saint Martin La Porte access adit (Lyon-Turin Base Tunnel). Completed installation of the yielding support system in stage 2 (30 m from the face). The deformable elements are visible in the shotcrete gaps. From Barla (2009).

This method implies the assessment of the rock mass properties in the "short" and "long term" conditions. This can be done based on the Geological Strength Index (GSI) proposed by Hoek & Marinos (2000 a, b). This index implies the assessment of lithology, structure and conditions of discontinuity surfaces and is estimated from the visual examination of the rock mass exposed in tunnel faces and in borehole cores. Experience shows that this approach in the case of squeezing ground is rather difficult and most of all uncertain to apply at the design stage. However, following tunnel excavation and based on back analysis of tunnel performance, one might be able to estimate the required parameters for final lining design (Hoek & Guevara 2009).

The tunnel response can be analysed by using the available analytical closed-form solutions and the convergence-confinement method or the more realistic simulations of tunnel excavation and reinforcement/support installation by using numerical methods such as the Finite Element or Finite Difference Methods. It is to be understood that the "short term" rock mass properties apply to the behavior of the tunnel during and shortly after excavation. The "long term" rock mass properties, which identify the material behavior contained in the plastic zone surrounding the excavation, imply the deterioration of the rock mass under high stresses and the occurrence of creep failure phenomena.

As demonstrated in recent papers (Barla et al. 2009, 2010; Sandrone et al. 2006), the most advanced approach to the analysis of tunnel performance in squeezing conditions, when severe to very severe squeezing problems are expected to occur (in line with the tunnel deformations shown in Figure 3.11), is to account for time dependence by using advanced constitutive models of the elasto viscous

plastic type with material parameters calibrated with reference to the in situ rock mass behavior.

These parameters are difficult to be found as in situ creep tests involve operational difficulties, and suitable scaling rules allowing for estimating them on the basis of laboratory data have yet to be validated. Nevertheless performance monitoring and back analysis may be adopted systematically, with convergence and stress measurements providing the appropriate input data, as demonstrated below in the case of the Lötschberg Permo-Carboniferous trough section and of the Saint Martin La Porte access adit.

In the case of the Lötschberg Base Tunnel the elasto-viscoplastic model proposed by Fritz (1984) was used by Sandrone et al. (2006). The results of a back analysis of convergence measurements in the East tunnel are plotted in Figure 3.18 versus time. It is noted that in this case a curve fitting procedure was applied based on the available analytical closed form solution for a circular tunnel in axisymmetric conditions developed by using the Fritz model.

In the case of the Saint Martin access adit along the Lyon-Turin Base Tunnel two constitutive models were adopted such as the 3 Stages Creep model (3SC) due to Sterpi & Gioda (2009) and the Stress Hardening ELasto VIscous Plastic (SHELVIP) model developed by Debernardi & Barla (2009). These models need a higher number of parameters, which may appear as a draw back for application in the field.

The two latter models have been tested first to verify their effectiveness in reproducing creep at the laboratory scale. Several triaxial creep tests on rock samples of various nature have been considered to this purpose, and among them also samples of coal taken from the Saint Martin La Porte access adit (Barla et al. 2007; Debernardi 2008) to verify their effectiveness in reproducing the phenomenon observed at the laboratory scale. As an example, Figure GB10 shows a comparison between the experimental and numerical results obtained from a multistage creep test on a coal sample. The agreement is shown to be rather satisfactory for both models.

The two models were then used to analyze the Saint Martin La Porte access adit response in terms of convergences monitored during excavation in the cross section at chainage 1444 m. The analyses have been performed with the Finite Difference Method and FLAC code (Itasca 2006) for the SHELVIP model and with the Finite Element Method and the SoSIA code (Gioda & Cividini 1996) for the 3SC model.

Axisymmetric conditions have been adopted in both cases in order to reproduce the three-dimensional influence of the tunnel face during excavation, which is known to play a significant role in squeezing conditions. The tunnel cross section is assumed to be circular. The total size of the two models is very large in order to minimize the boundary effects that are very significant in the case of large deformations as occurring in squeezing ground. Particular attention was paid in both cases to the description of the chronological sequence of excavation, pre-reinforcement and support placement.

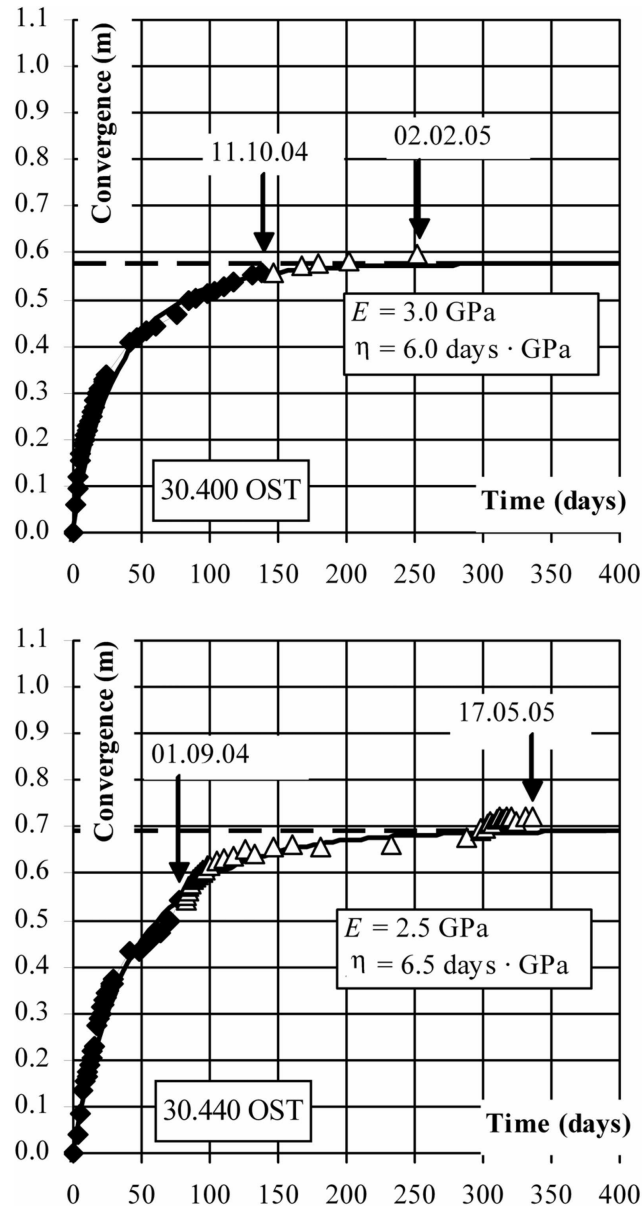

Figure 3.18. Lötschberg Base Tunnel: comparison of monitored and computed convergences based on the Fritz elasto-viscoplastic model in the East tunnel. From Sandrone et al. (2006).

As illustrated in Figure 3.20, the comparison of the numerical results in terms of the mean curve representing the radial displacements around the tunnel versus time and the monitoring data is rather good for both constitutive models, notwithstanding the scattering of the monitored values due to the high heterogeneity and anisotropy of the rock mass being considered.

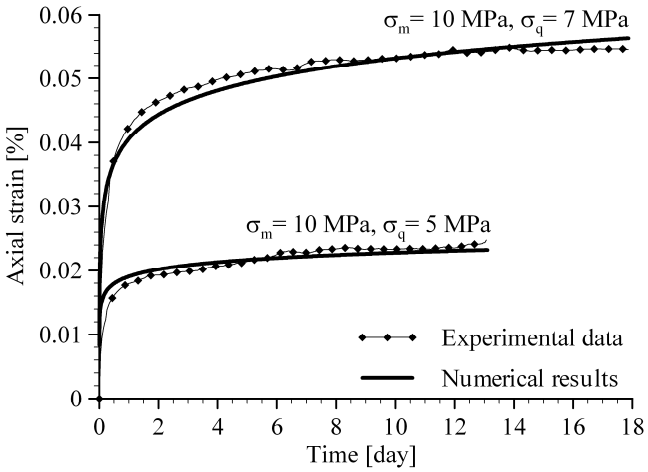

(a) SHELVIP model

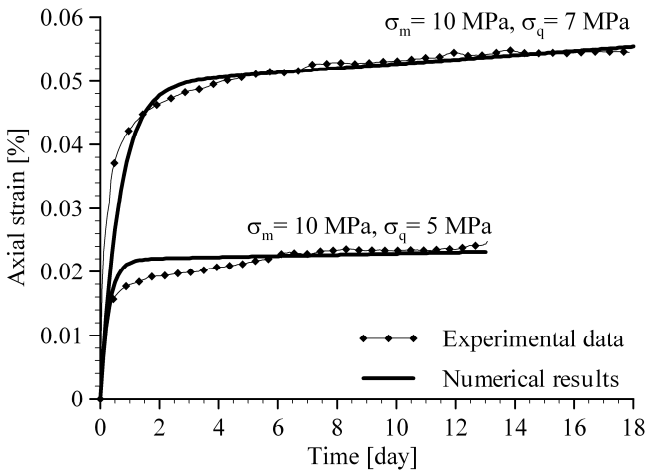

(b) 3SC model

Figure 3.19. Saint Martin La Porte access adit (Lyon-Turin Base Tunnel). Calibration of the SHELVIP and 3SC constitutive models on the results of a multistage triaxial creep test on coal. From Barla et al. (2009).

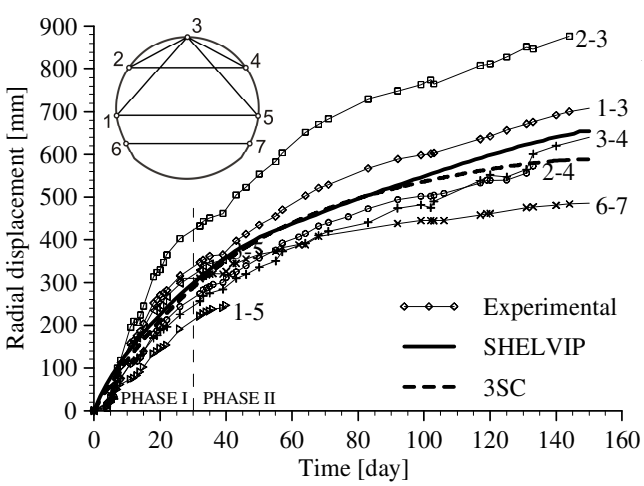

Figure 3.20. Computed versus monitored radial displacements with time, chainage 1444 m: SHELVIP model (solid line) and 3SC model (dashed line). From Barla et al. (2009).

3.2.5 *Open Issues*

It is demonstrated that the excavation of tunnels in squeezing ground with severe to very severe problems can be carried out successfully by using conventional methods and the available options for coping with such problems as illustrated above. Conversely, the use of tunnel boring machines in such conditions is yet under discussion due to the negative experiences which resulted in cases in very low rates of advancement and even in standstill with complete loss of the TBM (Barla & Pelizza 2000).

It is understood that in the case of Alpine base tunnels the systematic adoption of mechanized excavation would contribute significantly to savings in construction time and costs. Thus the question of TBM applicability in squeezing conditions associated with long deep tunnels is of significant interest and specific problems are being discussed in view of identifying the possible countermeasures to be applied in order to cope with such conditions.

3.3 *Spalling and Rock Bursting*

3.3.1 *Hazards and Levels of Spalling*

Nearly a half century ago, mines in South Africa began to experience a form of rock damage called spalling in which apparently intact rock walls fractured into parallel sheets and disintegrated under high stresses (Stacey & De Jong 1977; Fairhurst & Cook 1966). As mines around the world dug deeper in search of minerals, this failure mode became common place. It is now also a challenge in deep alpine tunnels. Escalating levels of spall damage in a TBM context are shown in Figure 3.21. This process can generate damage which ranges from a nuisance to a major source of overbreak and delay.

This failure mode can create a significant safety hazard for workers immediately behind the shield. While spalling normally develops within 1 or 2 tunnel diameters, interaction with subtle structure in the rockmass can lead to delayed release of spall damaged ground. In extreme cases, this delayed release can be associated with significant energy release in the form of a strain burst (Kaiser et al. 1996) as shown in Figure 3.21f. Significant spalling and bulking within the TBM shield can lead to issue of safety and jamming of the shield (Figure 3.22).

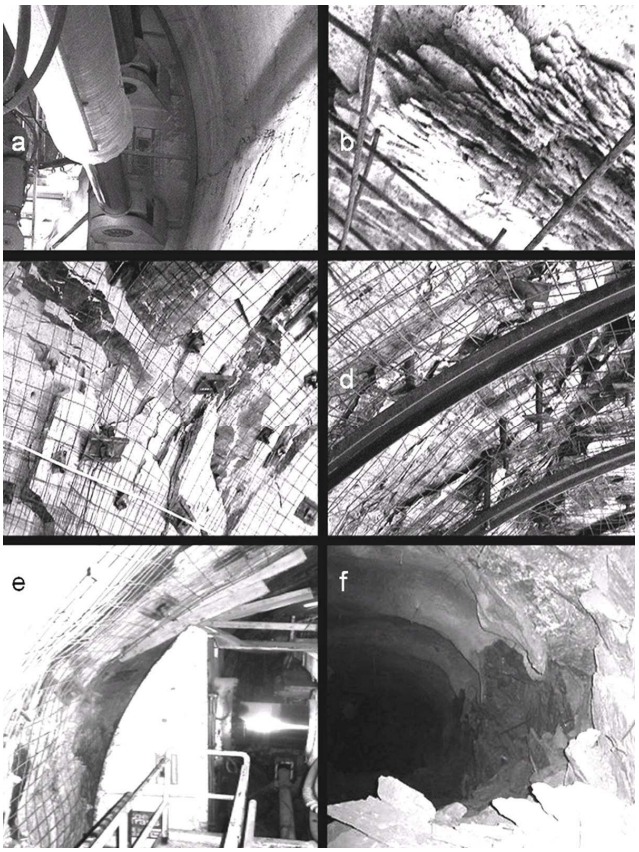

Figure 3.21. Increasing levels of brittle spalling and operational difficulty: a) spall initiation (small flakes on the wall); b) spall sheets of grain thickness penetrating into wall; c) Parallel wall slabs of cm thickness; d) significant overbreak and support challenges related to spalling failure; e) severe operational issues (gripping) associated with metre scale overbreak; f) strain bursting of spall damaged ground due to high stress ratio and buckling instability.

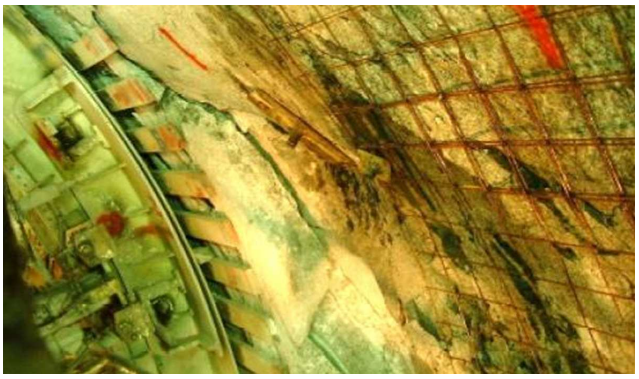

Figure 3.22. Spalling and energetic slab generation in gneiss behind TBM shield. Lötschberg Base Tunnel. From Vuilleumier & Seingre (2004).

Not all spalling is violent or leads to rockbursting. There is relatively little energy involved in the extension cracking process that leads to spalling. Individual flakes can be progressively ejected with some velocity, enroute to significant overbreak (Figure 3.23) but overall energy is typically manageable. The process of spalling, if moderate in extent, is not likely to damage robust TBM components although this ejection of small pieces can cause injury.

Figure 3.23. Progressive spalling above a TBM in granite.

The spalling process typically occurs within one to two diameters of the face and often within the shield zone of the TBM (Figure 3.22). Unlike the process of ductile shearing typical of squeezing ground (Figure 3.24), spalling involves the creation of boundary parallel extension fractures.

If constrained, these fractures may subsequently buckle in a violent fashion (Figure 3.25b). If the fractures are intercepted by an oblique joint, they may burst into the opening violently as energy due to bulking is released along the joint (Figure 3.25c). If the depth of spalling is sufficient to create a notch-like damage zone, the failure mode within the rock can transition to dilational shear at the notch tip creating additional bulking and outward pressure that may overcome support capacity in a violent strain burst (Figure 3.25d).

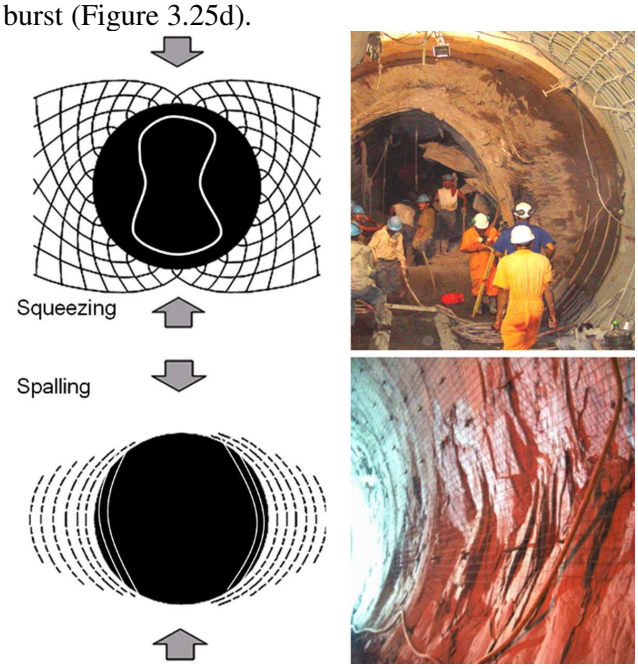

Figure 3.24. (top) Conventional assumptions of plastic shear with example from Yacambu tunnel in Venezuela; (bottom) Spall fracture geometry (Lötschberg Base Tunnel).

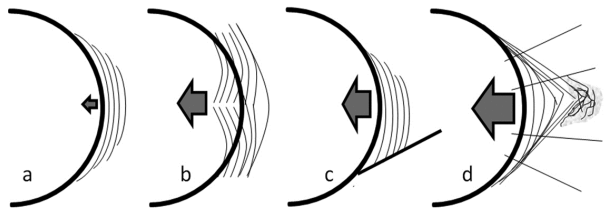

Figure 3.25. a) non-violent progressive spalling; b) violent buckling of spall conditioned rock (burst); c) release of dilatant spalling along joint (burst); d) transition to dilational shear at depth leading to support failure (burst).

Spalling can lead to bursting in the face of a tunnel. The flat shape of the tunnel and the sharp corner geometry at the face perimeter can lead to a substantial build up and sudden release of considerable strain energy leading to violent ejection. The spalling process can also interact with face-parallel foliation in metamorphic rocks to increase the problems encountered.

3.3.2 *Spalling and Rockburst Support for TBMs*

It is difficult to prevent spalling in a TBM tunnel. Proper support immediately behind the TBM shield (or immediately after each round in a drill and blast tunnel) is important however, to ensure worker safety and reduce the impact of spall-generated overbreak. A complete support package includes a strong mesh or screen to retain material, firmly and frequently anchored by bolt plates, straps and/or arch segments. Full steel arches are not always required or desirable but partial arch segments bolted into the rock provide effective holding capacity for the mesh retention system. The arches or arch segments need not be heavy - rather a light C-channel system is often effective. Grouted rebar can provide enough internal stiffness to reduce the propagation of fractures within the rock although their stiffness may result in internal rupture (with the remaining grouted segments performing an internal reinforcement function. A complete bolting pattern should, however, include a bolt with significant displacement capacity such as high strength Swellex or cone-anchor grouted bolts (Kaiser et al. 2000).

For open TBM's, a few critical elements must be present behind the shield for effective spalling and bursting control. First, there must be capability for bolting immediately behind the shield covering as much of the tunnel perimeter as possible (Figure 3.26a). The TBM can be fitted with a finger shield for worker protection (Fig. 3.26b) provided the fingers are stiff and the gaps between them can accommodate the installation of bolts and plates as needed. The ability to install steel rings or ring segments is useful. If wall bolting is needed (normally for high vertical stresses) then the grippers must be designed to pass over bolts and/or ring segments (Fig. 3.26c). Strong steel mesh should be placed above the steel arch segments with the mesh and the arches bolted to the rock (Fig. 3.26d). An alternative to mesh can be a system of longitudinal "straps" fabricated out of rebar as shown in Figure 3.26e.

Shotcrete sprayed over mesh with additional bolting through the shotcrete can add to the resiliency of the system, although stiff shotcrete applied on its own without additional support may make matters worse in this environment (Kaiser et al. 1996).

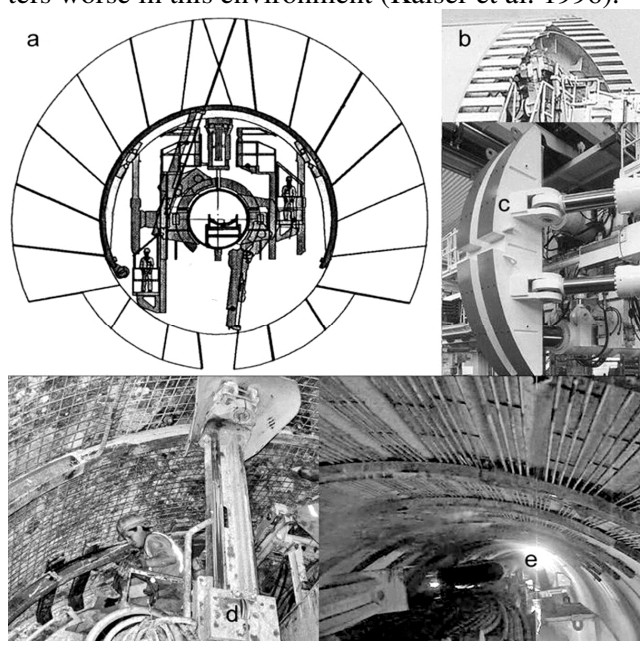

Figure 3.26. a) Complete bolting array behind TBM shield; b) short, stiff finger shield with spacing between fingers for bolting; c) gripper slots to fit over support elements; d) screen behind circular steel arches; e) welded rebar straps behind c-channel segments bolted to rock.

3.3.3 *Spall Prediction*

Conventional rock mechanics constitutive models used for excavation analysis have proven to be physically incorrect (Pelli et al. 1991) and unable to simulate this process, primarily due to the contrasting mechanics illustrated in Figure 3.24.

Numerous tools have been developed in succession, from empirical charts relating stress to strength, to simplified empirical criteria for use with elastic stress models, to practical phenomenological yield models for use with conventional non-linear analysis programs. Recently, fracture mechanics and discrete element simulations have drawn together and are moving towards a more physically rigorous solution. In practise, however, before relying on these more sophisticated techniques, it is critical to determine the mechanistic limits to the spalling process. Uniaxial and confined strength tests on hard rocks results in a non-linear envelope that can be described by a number of yield criterion including Hoek-Brown (Hoek et al. 2002), for example.

It is recognized, however, that the upper bound for rock strength in situ, away from the excavation and under higher confining stresses is the crack

damage limit (CD), a yield envelope typically 70-90% lower than the peak lab strength. At this yield threshold, accumulating cracks interact with each other and coalesce (Diederichs 2003, Martin 1997). This envelope is shown in Figure 3.27.

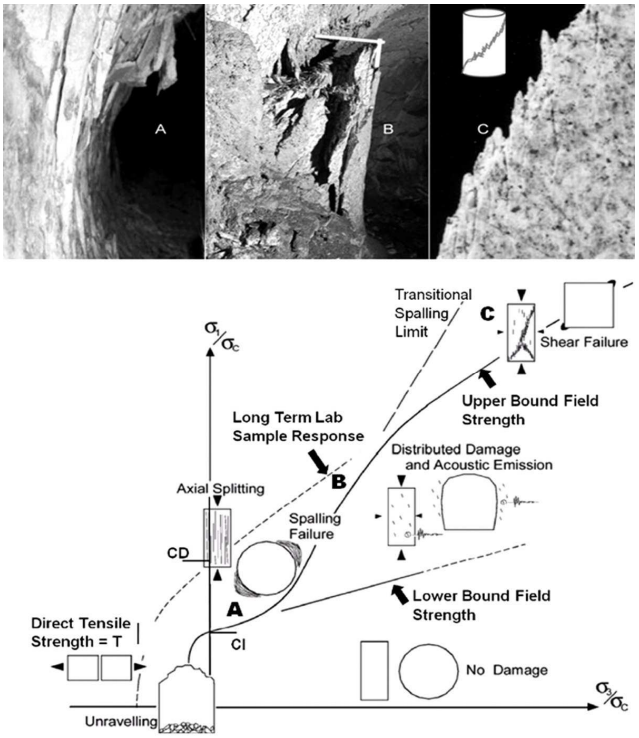

Figure 3.27. Composite strength envelope (from Diederichs 2003) showing transition between spalling behavior (A) controlled by the lower bound CI (damage initiation) through transition behavior due to geometric or stress confinement (B), to shear zone genesis due to crack coalescence (C) corresponding to long term lab strength controlled by crack interaction or critical damage (CD).

The lower bound for in situ rock strength at low confinements near excavation boundaries is given by the crack initiation limit (*CI*), obtained in the lab through acoustic or lateral strain measurements (Diederichs et al 2004). This stress limit corresponds to the observed onset of wall fracturing at stress levels only 35-50% of compressive strength of the rock. The transition between these two bounds is confinement and geometry dependent (*spalling limit*). At the tensile end of the confinement range, spall fractures is also sensitive to the true tensile stress limit for the rock mass. Under high confinement there is an upper bound to the stress levels at which spalling dominates and beyond which shearing and crushing take precedence (Diederichs 2003).

Not all rocks or rock masses are predisposed to spalling as a dominant mechanism. Conventional compressive failure in rock and soil mechanics is modelled as a shear process. For rocks to spall, they must be more prone to extension fracturing (tensile cracks) than to the development of shear planes and shear fractures. The latter is certainly the case in weak rocks and soil. This mechanistic limit is related to the ratio of *UCS* to *T* (true tensile strength or "Brazilian" tensile strength) but has many other influence factors. Typically, rocks with a UCS/T ratio less than 10 are unlikely to spall while ratios above 20 indicate a spall prone rock. Rocks between these limits may spall if the rock is massive and unweathered.

In general rock masses which are above a limiting intensity of jointing and which may be highly altered/weathered at the grain scale, may also be prone to shearing rather than spalling. GSI or RMR 60 is a reasonable lower bound rock quality for spalling to be likely and the process dominates at RMR values above 75 for hard rocks at depth (Diederichs 2007).

3.3.4 *Spalling Strength Thresholds*

The upper and lower bounds for tunnel wall strength can be obtained from uniaxial laboratory tests as illustrated in Figure 3.28. *CI* represents the stress level at which grain scale cracks begin to nucleate within the sample. This threshold can be detected using acoustic emission monitoring of lab samples as demonstrated in Diederichs et al. 2004. *CI* is the first point at which a systematic increase in crack emissions follows an increase in applied stress. In strain based monitoring, *CI* is also the first point of lateral strain non-linearity (Figure 3.28). Care should be taken as crack closure strain anomalies may overlap damage initiation strain readings, especially for damaged samples.

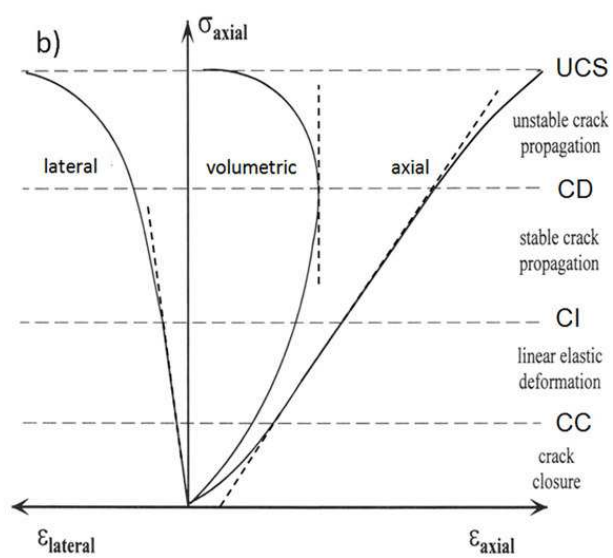

Figure 3.28. Crack thresholds from strain measurements.

CD, the upper bound field strength threshold, corresponds to the true yield stress in testing (critical crack damage and interaction). Martin (1994, 2007) suggested using the point of reversal in volumetric strain (transition from contraction to expansion). The crack damage threshold is also apparent from acous-

tic monitoring recorded during sample testing. The total hit count dramatically increases at *CD*.

3.3.5 *Empirical spall prediction*

Once *CI* has been determined and spall sensitivity has been assessed, it is possible to empirically predict the onset of spalling from Figure 3.29.

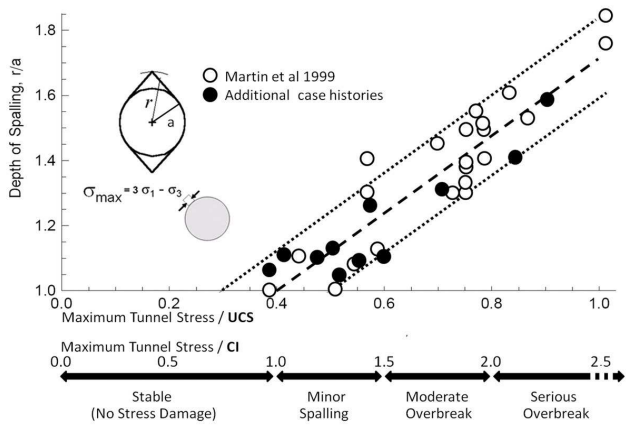

Figure 3.29. Empirical spall prediction based on CI (Martin 1999 updated by Diederichs et al 2010).

Where *CI* is known, a very preliminary approximation of overbreak extent measured as a radial distance from the tunnel center, *r*, is given (for a tunnel of planned radius, *a*):

$$\frac{r}{a} = 0.5\left(\frac{\sigma_{\max}}{CI} + 1\right) \qquad for\ \sigma_{\max} > CI$$

Using this simple predictor and based on assumptions of in situ stresses along a tunnel route, for example, the location and extent of spall-based overbreak can be estimated at an early stage of a project (Figure 3.30). It is important to avoid using too conservative an estimate of CI as the average value for systematic crack initiation already represents a reasonable lower bound for the purposes of this prediction.

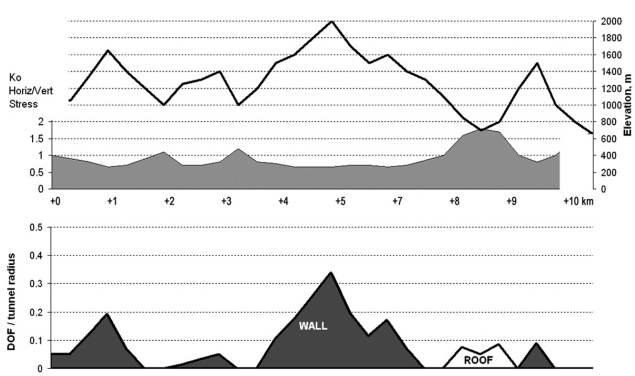

Figure 3.30. Utilization of a simple overbreak predictor for a tunnel in the Western Alps. The vertical stress and an estimation of horizontal stress (from regional modelling) are used in conjunction with Figure 3.29 to create a preliminary prediction of maximum anticipated overbreak.

The empirical technique can be extended using the above equation, or using the relationship for the CI envelope shown in Figure 3.27, combined with elastic modeling. Contours of FS=1 using either envelope or equivalent (Figure 3.29) give a very rough estimate for the extent of damage and the areas affected. This can be useful for 3D elastic modeling of intersections or complex geometries.

3.3.6 *Phenomenological Spall Modelling*

Ultimately, this failure mode must be analyzed in a non-linear fashion. This process is complex, since it involves a transition from continuum to discontinuum behavior. Models involving combinations of discontinuum and fracture propagation capabilities are under development to address this transition, although they are not yet commercially available to the practicing engineer. First, a practical tool for spall initiation and extent prediction using commercial continuum codes will be discussed here, mindful of the limitations.

Figure 3.31 illustrates the use of the spalling model presented in Figure 3.27 in a finite element program (PHASE2 - rocscience.com) that accepts "peak" and "residual" shear parameters as input. "Peak" represents the damage initiation threshold (CI) while "residual" represents the spalling limit (transitional behavior to high confinement shear). Shear at high confinement (at CD) is not correctly simulated in this model so the use is limited to near-excavation analysis. At low confining pressure the behavior after damage (yield in the model) is brittle with strength dropping to the spalling limit. At higher confinements, the behavior is strain hardening such that the model will show damage indicators but the ultimate rupture strength increases to the transitional envelope.

This approach can be implemented in commercial analysis programs using the generalized Hoek-Brown criterion:

$$\frac{\sigma_1}{UCS} = \frac{\sigma_3}{UCS} + \left(m\frac{\sigma_3}{UCS} + s\right)^a$$

The following procedure (Diederichs 2007) can be used to model spalling failure in a Hoek-Brown formulation (inelastic) with reference to Figure 3.28:

- Determine *CI* from lab data
- Set 'a' to 0.25
- Obtain a reliable estimate of tensile strength, T
- Calculate the appropriate 's' and 'm' for the "Initiation" envelope:

$$s_{CI} = (CI/UCS)^{1/a} \qquad m_{CI} = s_{CI}(UCS/|T|)$$

A transition envelope (Spalling Limit) can be approximated by setting a=0.75, s=0 (or slightly higher for numerical stability) and m=7 to 10. Note that the

upper bound (CD) is not modeled here as this criterion is only valid for near excavation (lower confinement) behavior.

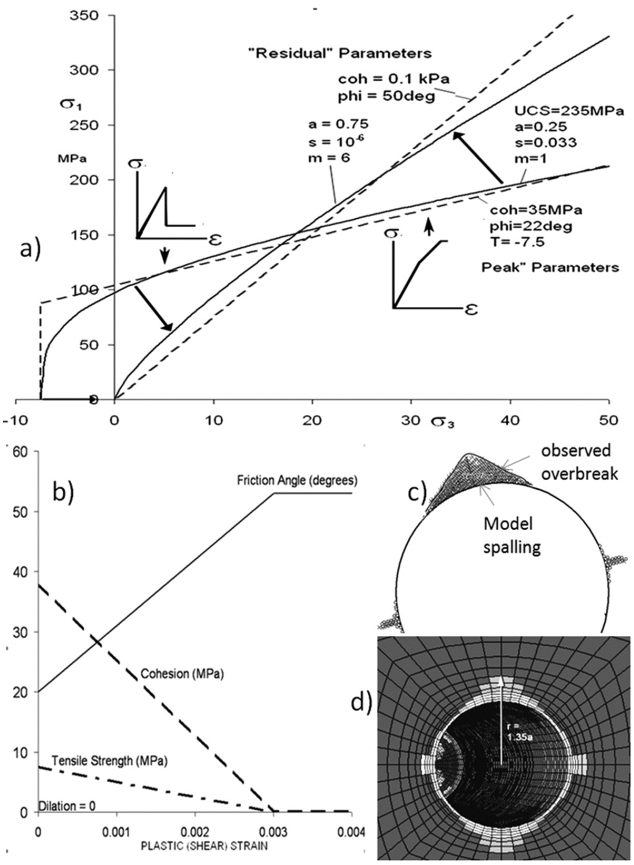

Figure 3.31. Modelling damage initiation and the spalling limits (c, d): (a) using "peak and residual" parameters (PHASE2) and (b) using "strain-weakening" model (FLAC). Plastic strain at final cohesion loss should not be less than 2CI/E for numerical stability.

This behavior can also be replicated in a model that has strain-modification of parameters such as FLAC (itascacg.com). Figure 3.31b shows the modification, with plastic strain, of friction, cohesion and tensile strength (linear parameters selected to match the non-linear modified Hoek Brown envelope in Figure 3.31a. Dilation can also be controlled although more research is needed to calibrate this behavior.

These models are useful for predicting the extent and final shape of spall related breakout (Figure 3.31c & d). They are not valid, however, for predicting post yield dilation, and therefore are inadequate for the design of passive reinforcement-rock interaction. This is complex as the dilation rate is both plastic strain dependent and is highly confinement dependent. If the depth of failure, DOF, can be determined, the inelastic wall displacement, WD, with modest support pressure, P (distributed surface restraint pressure), can be predicted from the empirical formula (simplified from Kaiser et al 1996):

$$WD = DOF\left(0.3e^{-P/70}\right)$$

While the methodology described above was developed and calibrated for a granite/granodiorite tunnel, this approach has been shown to be representative of actual behavior in a highly consolidated massive mudstone (Figures 3.32 and 3.33).

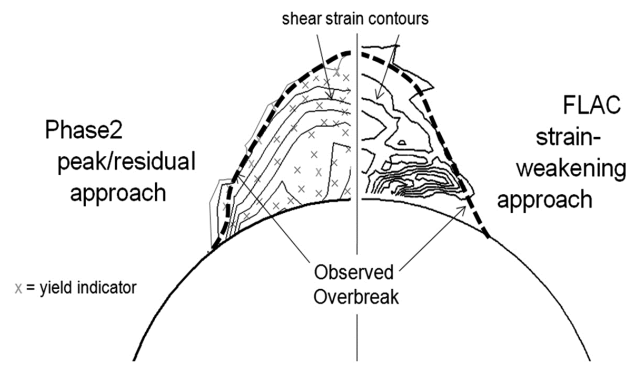

Figure 3.32. Comparison of spall damage and overbreak prediction for a large TBM tunnel in overconsolidated (low porosity) mudstone. Contour lines indicate significant (order of magnitude) increase in shear strain beyond elastic background.

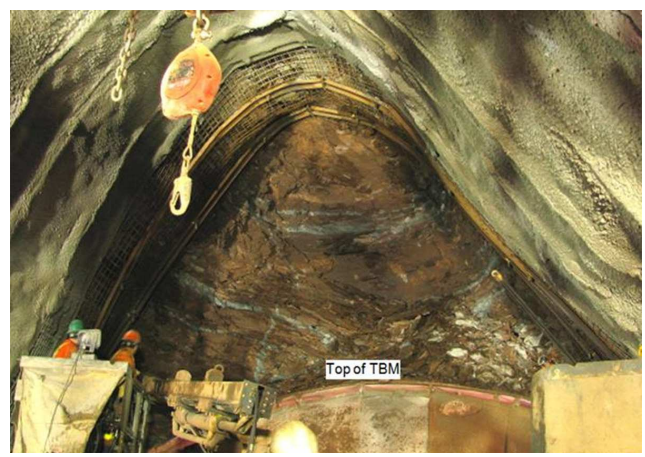

Figure 3.33. Overbreak from tunnel roof in Figure 3.32.

3.3.7 *Open Issues*

It is important to recognize that there are limitations to this continuum approach. The methodology described above is robust in its ability to predict the onset of damage, the extent of damage (yield indication) and failure (elevated shear strain). It is also reliable in its ability to predict the location and shape of the spall damage zone. It is currently not capable of predicting:

- Dilation rate during spalling, as a function of total plastic strain and confinement
- Ultra-sensitivity of crack propagation to modest support pressures
- Transition from spalling to strain-bursting
- Time dependency and other sensitivities.

More sophisticated continuum-discontinuum codes (Figure 3.34) currently under development promise to address these shortcomings and improve spall prediction and support design in these environments.

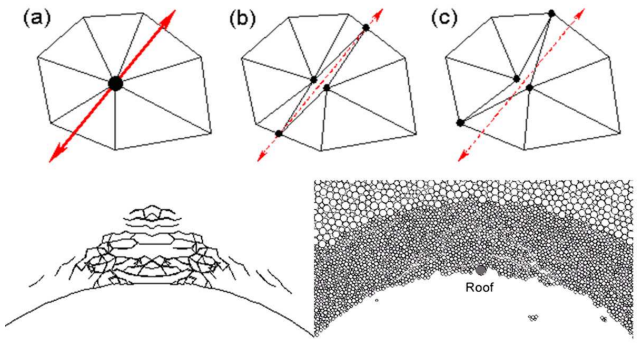

Figure 3.34. Top: Process of continuum-discontinuum within a finite-element/discrete element hybrid model: a)maximum local principal stress within a model. b) New fracture parallel to maximum compression (remeshing required after fracture formation). c) fracture along pre-existing boundary. From Vyazmenski et al. (2007). Bottom left: FEM-DEM results with induced fracturing and remeshing. From Coggan et al. (2003). Bottom right: Bonded disc model for rock fracture. From Tannant & Wang (2004).

3.4 *Water Inflows and Rock Mass Drainage*

3.4.1 *Hazards related to water inflow and rock mass drainage*

In Alpine tunneling groundwater related problems can be very severe and have caused substantial delays and cost overruns in past projects (e.g. Simplon Base Tunnel, Lötschberg Crest Tunnel, Furka Base Tunnel). Due to the high depth and water pressures all traffic tunnels in the Alps are constructed as drainage systems, sometimes with reduced inflows by grouting the rock mass around the excavation. Groundwater related problems can be direct or indirect and subdivided into 5 categories:

1. High water inflows causing excavation and safety problems
2. High water pressures and seepage forces causing instability problems
3. High water inflows causing impacts on surface springs and wetlands
4. High water inflows causing settlements of sensitive surface layers (soils)
5. Deep tunnel drainage and pore pressure drawdown causing large scale rock mass deformation.

Under special conditions water inflows to deep underground excavations in rock can reach several m^3 per second. If these high rates can not be drained efficiently, the underground excavations can become partially or completely flooded (Fig 3.35). Tunnel inflows are often sudden and sometimes violent, especially when an underground excavation is drilled from a low permeability section into an aquifer or into a highly conductive water conduit, such as an open karst pipe or fracture with high fluid pressure.

Mainly in sedimentary rock formations or in fault zones, aquitards of limited thickness can be loaded with high fluid pressures from nearby undrained aquifers, leading to hydraulic ground failure around the excavation. On the other hand high fluid flow velocities near excavation boundaries lead to high seepage forces, for example in cataclastic faults or on fracture surfaces, inducing shear failure.

Figure 3.35. Partially flooded Simplon tunnel at chainage 4500. From Kovari & Fechtig (2000).

Strong water inflows to deep tunnels can also lead to significant reductions in far field pore pressures and groundwater table elevations. Such near surface pore pressure changes influence the discharge of springs and can induce strong settlements in fine-grained or organic soils. On the other hand also deep tunnels without large inflows cause very strong pore pressure reductions at late times. At steady state these pore pressure reductions can impact kilometer large areas with large scale settlements of up to decimeters even in hard rocks (e.g. Loew et al. 2007, Zangerl et al. 208 a,b). Successful management of these hazards requires a comprehensive understanding of the hydrogeological situation and underlying mechanisms.

Stini (1950) has developed useful conceptual models for tunnel inflows in various hydrogeological environments. Three main types of hydrogeological settings have to be distinguished: groundwater flow in crystalline rocks (dominated by flow in fractures and phreatic water tables), flow in sedimentary sequencies composed of aquifers, aquitards and aquicludes (dominated by fracture or porous media flow, and partially confined or artesian pressure conditions), and flow in karst systems. The characteristic spatial and time-dependent distributions of groundwater flows in such systems form the basis for inflow predictions and quantitative analyses. The

basic properties of these different hydrogeologic environments are described in the following sections.

3.4.2 *Spatial and temporal distribution of tunnel inflows in fractured rocks*

In crystalline rocks (magmatic and medium-high-grade metamorphic) brittle fracturing is the principal parameter regulating tunnel inflow rate and dominates over depth and lithology (e.g. Long et al. 1991, Stober 1995, Caine and Tomusiak 2003, Masset and Loew 2010). The transmissivity of individual fractures is spatially variable, channelized (e.g. Moreno and Neretnieks 1993) and stress dependant (e.g. Barton et al. 1995). Masset and Loew (2010) have analyzed water inflows from 23 tunnels and galleries, 136 km in length and located in the Aar and Gotthard massifs of the Swiss Alps. Here the highest early time tunnel inflow rate is 1,300 liters per second (l/s) and has been reported from a shallow hydropower gallery intersecting a 200m wide cataclastic fault zone. From back-analysis of 1,361 tunnel intervals with a length of 100m, a lognormal transmissivity distribution could be derived, with interval transmissivities ranging between 10^{-9} and 10^{-1}m²/s within the first 200-400m of depth and between 10^{-9} and 10^{-4}m²/s in the depth interval of 400-1,500m below ground surface (Figure 3.36). Outside brittle fault zones, a trend of decreasing transmissivity/hydraulic conductivity with increasing depth was observed for schistous and gneissic units, whereas no trend was identified for the stiffer granitic rocks.

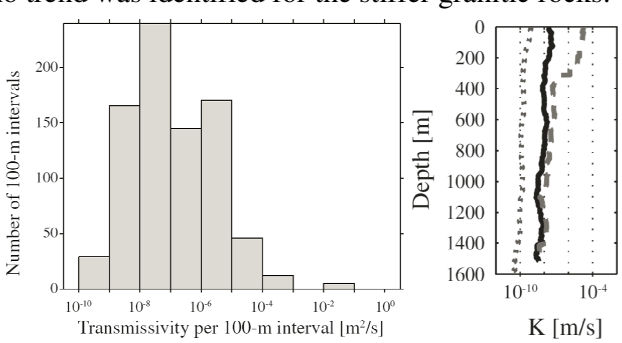

Figure 3.36. Transmissivity and hydraulic conductivity distribution derived from inflows to 100 m long tunnel intervals in the crystalline basement rocks of the Central Alps. From Masset and Loew (2010).

In fractured sedimentary rock sequences, which are not dominated by karstification, the role of tectonic fracturing on tunnel inflow can be significantly reduced compared to the impact of hydrostratigraphy (see e.g. Stini 1950) and lithology. As shown in Section 2.2.1 subhorizontal sequencies of aquitards and confined aquifers (Wildhorn Nappe in northern part of Lötschberg Base Tunnel) can lead to a substantial reduction in tunnel inflow, while phreatic or inclined sedimentary aquifers which are directly recharged from ground surface or overlying Quaternary aquifers (Doldenhorn Nappe in central part of Lötschberg Base Tunnel) can have very high long term yields. Within a given formation, fracturing, mineralogy and sedimentary sequences (i.e. bedding heterogeneity) play an important role for the effective hydraulic conductivity, which is often strongly anisotropic.

Transient tunnel inflow from fractured rocks strongly depends on tunnel depth (e.g. Loew et al. 2007). In the upper 200-400 m below ground surface, Alpine valleys slopes often show fractured rocks with high fracture frequency and aperture (due to unloading, landsliding and weathering effects). Extreme cases are reported from slopes with block or flexural toppling (e.g. Loew et al. 2007). The hydraulic conductivity in these regions is increased by several orders of magnitudes (Masset and Loew 2010) and leads to very large initial tunnel inflows, strong water table drawdowns down to the tunnel elevation, and late time inflows which are directly controlled by groundwater recharge at ground surface (mainly from snow melt and summer rain storms).

Transient tunnel inflows from fractured rocks at greater depth only show strong variations at early times. These initial transient inflows always decrease with time. During the first hours to days, bleeding of fractures with limited extent (water released from storage in intersected fractures) or closure of fractures (from the reduction of pore pressures) often leads to a so-called flush flow period with strongly decaying inflow rates (Moon & Fernandez 2010). Most inflows that survive this period initially decrease proportional to the logarithm of time and stabilize after a few weeks to months.

3.4.3 *Spatial and temporal distributions of tunnel inflows in karstified rocks*

Karstified rocks develop from chemical dissolution of carbonates or sulfates at ground surface and at depth. Gypsum and anhydrite dissolve in pure water; carbonates require water and a dissolved acid (mainly CO_2). The main factors driving karstification in carbonates are rock mineralogy, CO_2 partial pressure and temperature. Dissolution of carbonate minerals decreases in the following order: Mg-Calcite, Calcite, Dolomite. Rocks which contain silicates and fine grained minerals are less prone to karstification than pure and coarse grained carbonates.

In active karst systems dissolution voids are progressively widening in response to concurrent hydraulic boundary conditions, and are not filled with substantial amounts of dissolution residue or allochthonous sediments. The most important boundary conditions for active karst systems are the terrain surface, the elevation of the receiving stream and important aquitard boundaries. Mature karst systems are composed of an epikarst layer close to the terrain surface, a transfer zone and the karstic base level close to the elevation of the receiving stream (Figure 3.37).

In fossil or paleo-karst (Bosak et al. 1989) the dissolution voids are often filled with sediments because the groundwater flow in these systems has been interrupted as a result of changing hydraulic boundary conditions at ground surface. In Alpine settings old karst systems have been observed as cave systems above the current level of the receiving streams or as sediment filled (clogged) pipes below the level of the current receiving streams. This implies that the prediction of karst water inflows to tunnels does not only require studying currently active karst systems but also the long term geomorphological evolution of the project area.

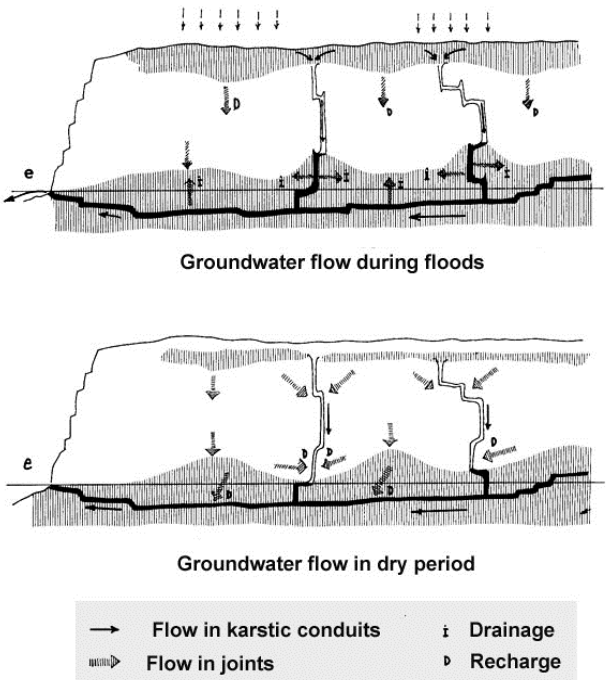

Figure 3.37. Recharge dependent groundwater flow in mature karst systems. From Therond (1973).

Palmer (1991) describes four morphological types of karst systems (Figure 3.38). If water infiltrates into carbonate rocks along discontinuities (mainly fractures, but also along faults and bedding planes) the conductive fracture sets are mirrored in the geometry of branchwork and network karst systems. Network systems form when recharge is diffuse and distributed (Clemens et al. 1997) - branchwork systems form when recharge is localized, for example in high-alpine regions. Anastomotic systems form when hydraulic gradients are small or soluble rocks occur within a plane. Ramiform and spongework systems are determined by endogenic dissolving agents (CO_2 and H_2S).

These fundamental concepts explain why tunneling projects in karst terrains are confronted with a large variety of tunnel inflow rates, dependant on the maturity, depth and age of the intersected karst system. Highest inflows are caused by open karst conduits of large diameters (meters) and/or a network of fractures widened substantially by dissolution. The complex transient tunnel inflow behavior is related to the fact, that water levels in karst systems change quickly and strongly in response to surface recharge conditions. The fluid flow interactions between the fractured rock matrix and the karst conduits change in response to the water table elevation (Figure 3.37): During flooding periods fast flow takes place in the transfer zone, fractures in the rock matrix are recharged, and water tables increase dramatically in the transfer zone. During dry periods slow leakage takes place from the rock matrix into the channels of the transfer zone and the water table comes close to the base level elevation. Inflows from deeper karst systems can increase with time due to continued erosion of sediment infills.

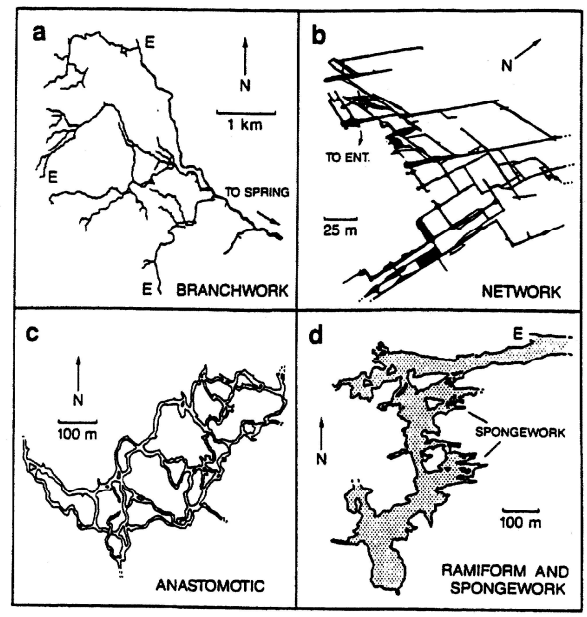

Figure 3.38. Four morphological types of karst systems. From Palmer (1991).

Initial tunnel water inflows from dissolution widened fractures in deep karst systems can reach up to 200 l/s and station (Simplon tunnel). Highest reported initial inflows from decimeter wide karst pipes in the Alps amount to 700 l/s (Rawil tunnel). One of the most dramatic case histories is the Karawanken tunnel (Schubert & Morinko 1989, Maidl & Handke 1993). Here the tunnel face collapsed in front of a fault zone with large karst cavities after a longer period with predrilling interventions. Predrillings often became clogged with soils and had already indicated very critical hydraulic conditions (pressures up to 16 bars, inflows up to 60 l/s, large forces on drilling rig pushing jumbo 30 m backwards). The sudden and violent collapse of the fractured tunnel face generated a flood wave of 1.2 meters height (assumed inflow rate 10’000 l/s) and the deposition of 1200-2000 m^3 of soil (mainly sand and gravel).

3.4.4 *Predicting groundwater inflow in fractured rocks*

The prediction of inflows to tunnels in fractured crystalline bedrock is strongly dependant on the spatial permeability distribution, which is very heterogeneous, potentially anisotropic, and ranges over many orders of magnitudes. It has been shown that the bulk tunnel inflows are controlled by very few highly conductive pathways (singular conductors) directly intersecting the excavated tunnel (e.g. Long et al. 1991, Masset & Loew 2010). In crystalline rocks such highly conductive pathways often correlate with the occurrence of persistent fractures in regions with low confining stress (typically shallow depth of 200-400 m, slopes with steep topographic gradients, slopes showing gravitational slope deformations, e.g. toppling) or with damage zones of brittle faults. In case of deep tunnels, the prediction of the specific locations and hydraulic properties of these singular conductors is far from trivial and requires systematic predrillings.

Modeled inflows to tunnels are always controlled by the assumed hydraulic conductivity distributions, which are very difficult to assess from ground surface. Therefore understanding the hydrogeological conditions and deriving statistically reliable information on the hydraulic conductivity distributions is much more important than any seemingly precise model prediction. Special attention should be given to the highly conductive pathways (singular conductors).

Groundwater flow around and into tunnels is mainly driven by gradients of hydraulic head which is composed of elevation head and pressure head. The hydraulic head at the boundary of an open tunnel normally corresponds to the tunnel axes elevation - the low atmospheric pressure head is often neglected. As the pressure head in a saturated formation is always bigger than the atmospheric pressure in the tunnel, every open tunnel laying in fully saturated groundwater generates water flow into the tunnel from all sides. Unsaturated conditions around deep tunnels can develop for various reasons, for example when higher conductivity layers around a tunnel are completely drained due to lack of groundwater recharge from the surrounding low conductivity medium, or by degassing of initially highly pressurized groundwater (Jarsjö & Destouni 2000).

Several 2-dimensional analytical models have been proposed to predict groundwater inflows to tunnels in fractured rock (e.g. Goodman et al. 1965, Zhang and Franklin 1993). Most of these models assume that, on the scale of hundreds to thousands of meters which is the relevant scale for tunnel construction and operation, the fractured rock mass can be approximated with equivalent continuum properties (e.g. Snow 1969). Alternatively these models can be applied to individual planar conductors, such as brittle faults or fault zones, with homogeneous transmissivity and no leakage. Such equivalent continuum hydraulic conductivities might be scale dependant (e.g. Clauser 1992). This implies that hydraulic data from lab or borehole tests must be treated with caution.

In case that the rock mass hydraulic conductivity can be described by an equivalent continuum, the flow geometry in crystalline rocks is less complex than in sedimentary sequences. Most crystalline bedrock aquifers can be treated as phreatic aquifers with depth-dependant hydraulic conductivity. The flow in sedimentary sequences, like the ones discussed in Section 3.4.1, is often partially confined or leaky. The corresponding flow models are more complex and rarely amenable to analytical solutions.

In fractured crystalline rocks, due to continued drainage of the open excavation, hydraulic head and pressure drawdown around a tunnel develop with time, and the flow geometry might significantly change. For analysis purposes the flow geometry can be classified into several stages when the flow field can be approximated by a simple pattern and analytical solutions applied (Loew 2002). All solutions are valid only for a vertical plane normal to the tunnel axes, i.e. all 3D effects close to the advancing tunnel face are not considered. All solutions assume homogeneous, but not isotropic hydraulic properties of the rock mass surrounding the tunnel and a uniform head distribution in the formation prior to the tunnel excavation (i.e. a flat groundwater table and no vertical head gradients).

The simplified flow patterns are illustrated in Figure 3.39. The first model represents infinite acting radial flow (Figure 3.39a) and is valid as long as the groundwater pressure drawdown around the tunnel does not intersect the groundwater table or any other boundary. For low permeability tunnel sections this situation holds for long periods of time (years). The second flow model is the steady state solution of the first model including a linear constant head boundary (Figure 3.39b). This model can be applied at later times and/or in a higher permeability environment, when a recharging lake or a prolific (Quaternary) aquifer at the surface is holding the water table at a constant level. The third model is a simplified solution for linear flow under a constant drawdown. It applies when the drying out of surface springs in direct response to the tunnel or gallery excavation demonstrates the drawdown of the water table down to the tunnel elevation and when linear horizontal flow normal to the tunnel axes is a reasonable approximation (Figure 3.39c).

The first stage with transient radial flow can be described by the well known asymptotic constant head test solution of Jacob & Lohman (1952):

$$Q(t) = \frac{4\pi KL(h_e - h_t)}{2.3\log(2.25KLt/Sr^2)}$$

where t is time, K is effective hydraulic conductivity in the radial flow plane, L is tunnel length under consideration, (h_e-h_t) is the difference between the initial formation head and the tunnel head (equal to the distance D between the tunnel and the groundwater table elevation) and S is elastic storativity (typically taken as 1E-6 m^{-1}, Masset & Loew 2010).

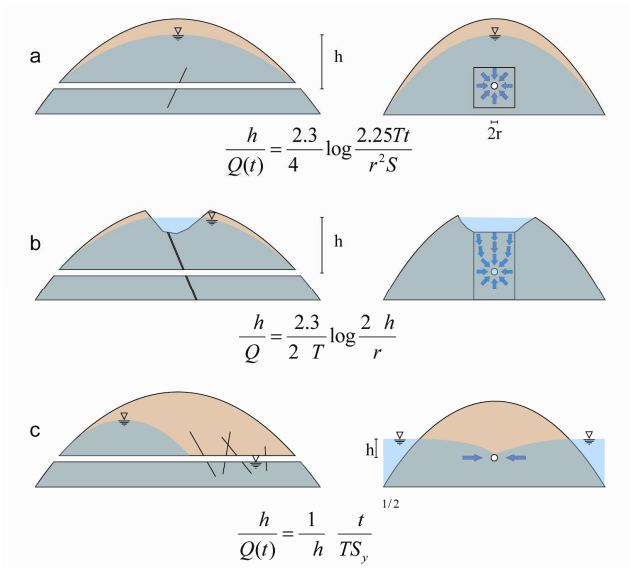

Figure 3.39. Stages of tunnel inflows in homogeneous rocks with simplified flow geometry.

When the head drawdown created by a deep tunnel (tunnel radius r << depth of tunnel below water table) reaches a stable and flat groundwater table, the flow converges towards a steady state flow field. The corresponding steady state inflow rate Q into a tunnel segment of length L can be described by the well known formula reported by Goodman et al. (1965):

$$Q = \frac{2\pi KL(h_e - h_t)}{2.3\log(2(h_e - h_t)/r)}$$

Lei (1999, 2000) has derived an analytical solution for the steady state head field and groundwater flow around a tunnel close to the surface assuming again a linear constant head boundary above the tunnel. El Tani (1999) gives approximate solutions for steady state inflow to tunnels with elliptical or square cross-sections. Zhang and Franklin (1993) have discussed the case of a deep tunnel in a rock mass with an exponential decrease of hydraulic conductivity with depth.

In case the drawdown reaches the tunnel elevation (Stage 3) approximate solutions are available for Dupuit horizontal flow. For a tunnel that fully penetrates such a zone Goodman (1965) derived an approximate solution for a parabolic drawdown surface:

$$V(t) = \left(\frac{8C}{3}K_x(h_e - h_t)^3 S_y t\right)^{0.5}$$

where V(t) is the integrated inflow rate (a volume) for a tunnel segment of unit length, and C is an experimental constant ranging between 0.5 and 0.75. An alternative model for this stage is the solution derived by Doe (1991) for linear flow under a constant drawdown (Figure 4.2c). The specific yield (S_y) in near surface crystalline rocks can be set to 0.01 (Masset & Loew 2010).

First order estimations of groundwater flow in horizontal and confined sedimentary aquifers can be made for the case when the flow pattern can be approximated by a superposition of linear horizontal flow with vertical flow to the tunnel. Kawecki (2000) has developed a set of equations for this case, which are based on approximations derived for horizontal oil wells in confined aquifers. The analytical equations can be solved iteratively (Kawecki 2000, Loew 2002).

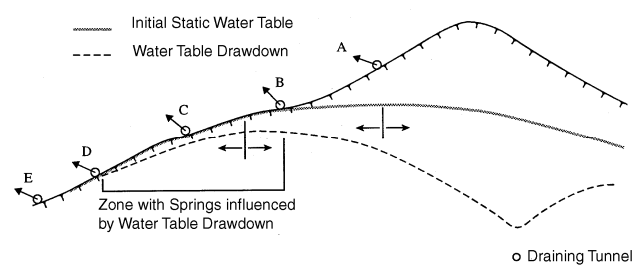

Figure 3.40. Impact of water table drawdown on surface springs.

A falling water table can have serious impacts on wetlands, creeks and springs. Major impacts have to be expected at locations where the static (natural) water table is close to the ground surface. Lowering such a water table will cause springs recharged from bedrock aquifers to run dry (Figure 3.40, springs B and C), or to become reduced in discharge (springs E and eventually D). Springs recharged by perched or near surface aquifers (such as slope deposits, A) are not influenced by a draining tunnel.

3.4.5 *Predicting groundwater inflows in karstified rocks*

Marinos (2005) gives a useful typology of tunnel inflows in karst systems. This typology relates to the location of the tunnel with respect to the epikarst, transfer zone and karst base level. As explained in Section 3.4.3 hydraulic properties of karst systems also change with time. As the precise localization of karst conduits or karstified fractures is not possible from ground surface, systematic predrillings are

necessary requirements in all underground constructions. Predrillings in deep tunnels are confronted with large fluid pressure gradients and have to be carried out with the necessary precautionary measures (standpipes with sufficient length and strength, blowout preventers).

Groundwater flow in open karst tubes of constant and diameter D can be described by (Strickler 1923):

$$Q = k_s \frac{\Delta h}{L}$$

where Δh represents head loss over the tube of length L, and k_s the coefficient of head loss, defined as:

$$k_s = \pi \frac{D^2}{4} K_s \left(\frac{D}{4}\right)^{2/3}$$

K_s is the Strickler coefficient typically taken as 20 (smooth tube surface: 15, rough tube surface 25). These equations can also be applied to karst systems composed of interconnected systems of single tubes as long as the tubes remain fully saturated.

3.4.6 *Predrilling and borehole testing during tunnel excavation*

The reliability or predictive power of predrillings depends on the target geometry (planar fault zone, fracture zone, linear karst conduit) and the type, number and location of predrillings. For linear karst conduits single predrillings are not sufficient for a reliable detection (Pesendorfer & Loew 2007). Multiple predrillings or drilling fans executed with the drilling jumbo increase detection reliability.

Predrillings can be used for new powerful borehole testing protocols (Pesendorfer & Loew 2010). For example, hydraulic tests carried out in open or packed-off horizontal predrillings can be used to get detailed information about the geometry of water conducting pathways (individual fractures, fracture networks, karst pipes) and their scale (i.e. distance) dependent hydraulic conductivities. Figure 3.41 shows an example from constant rate outflow and pressure recovery tests carried out in the Doldenhorn section of the Lötschberg Base Tunnel. The hydrotest carried out in borehole K8WC shows a perfect match with a simulation for a model composed of bilinear flow from a finite-conductivity fracture and a linear constant head boundary.

Such tests can also be carried out in combination with geophysical measurements, for example optical televiewer logging and single radar reflection measurements. Radar tests have been shown to be useful measurements for the detection of large karst cavities in limestones. Figure 3.42 shows the results of numerical simulations of a 0.5x5m wide karst cavity in homogeneous and heterogeneous limestone. According to these simulations and observations made in the Lötschberg Base Tunnel, karst cavities with such dimensions can be reliably detected within a radial distance of about 5 meters from the borehole (typical distance to tunnel excavation boundary).

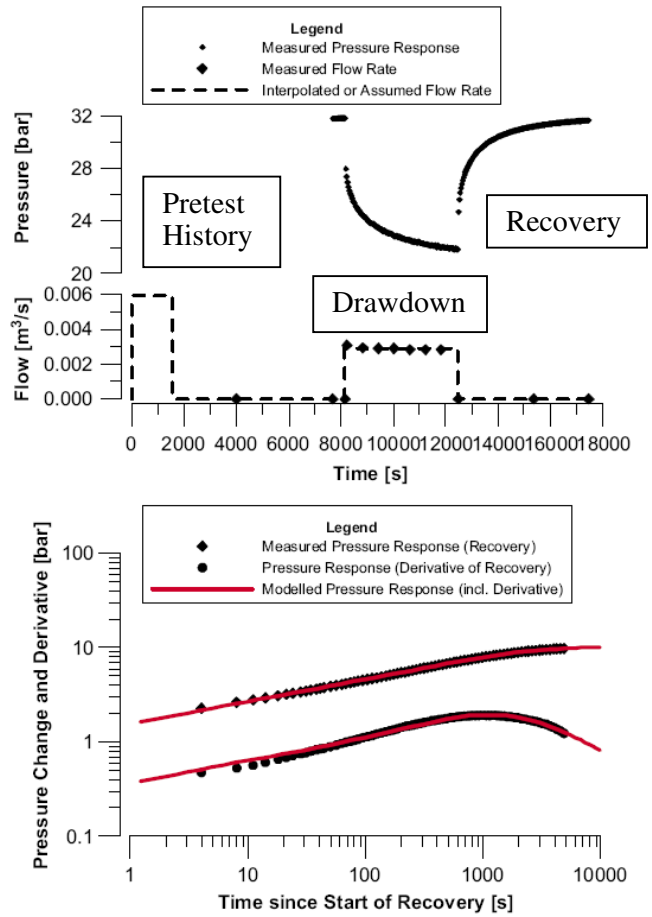

Figure 3.41. Flow rate and pressure history (top) of constant rate outflow and recovery test carried out in open predrilling (K8WC of Lötschberg base Tunnel, Doldenhorn nappe section). Analysis of pressure recovery and pressure recovery derivative (bottom) with log-log diagnostic plot and simulation results (red line). From Pesendorfer and Loew (2010).

3.4.7 *Open issues*

Today the spatial transmissivity distribution of fractured rocks cannot be reliably modeled or predicted with physical approaches. Also systematic probing from ground surface is not feasible for large and deep tunneling projects. Therefore, without systematic predrillings from the ongoing excavation, it is not possible to reliably predict the location of individual inflows, and professionals involved in the tunnel design should aim at describing inflow distributions for representative, i.e. km-long tunneling sections. The prediction of tunnel water inflows to such sections relies on a sound conceptual model for the hydrogeological framework, and a description of the hydraulic conductivity distribution of the water conducting features. However, fractures or karst conduits with very high transmissivity, which control the bulk water inflow, occur rarely and are often not sampled in site characterization programs. One option to overcome this problem is to fit appropriate (e.g. log-normal) distributions to the sampled con-

ductivity data and extrapolate the distributions to the non-sample tails (Raymer 2001).

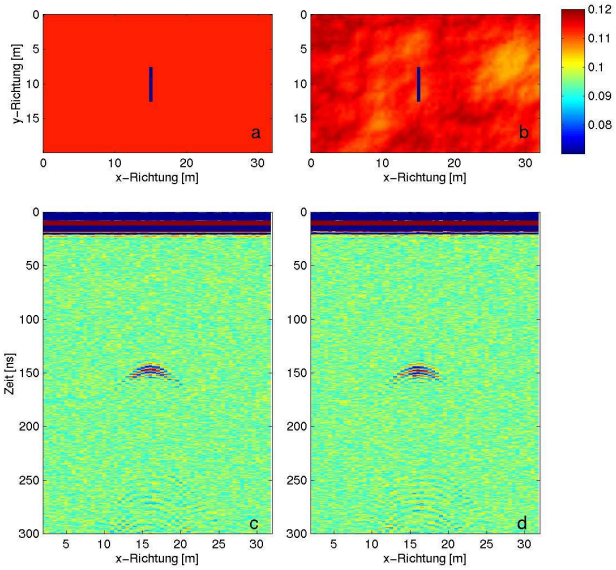

Figure 3.42. Simulation of single hole radar reflection measurements (bottom) in homogeneous (top left) and heterogeneous limestone (top right) with karst conduit of 5m*0.5m size. From Maurer et al. (2000).

When working with data from hydrotests in fractured rocks, a systematic comparison between hydraulic tests carried out in predrillings and subsequent tunnel inflows at the same locations show that hydraulic conductivity derived from predrillings is generally bigger than the values derived from back analysis of tunnel inflows at the same tunnel sections (e.g. Ivars 2006, Pesendorfer et al. 2010). In addition transient tunnel inflows from fractured rock masses generally decay more rapidly than predicted by the semi-logarithmic solution of Jacob & Lohman or numerical models that do not account for hydromechanical coupling (Figure 3.43).

Besides errors arising from the assumption of a homogeneous continuum with 2D radial flow, the solutions presented above for fractured rocks can yield misleading results due to boundary effects (e.g. permeable or conductive faults), stress-permeability coupling (e.g. closure of fractures), groundwater degassing (from groundwater with high contents of dissolved gases), temperature effects (e.g. temperature dependant water viscosity and hydraulic conductivity) and turbulent flow. As shown by Ivars (2006) with 3DEC model simulations, stress-permeability coupling can be considered as one of the main causes for the reduction of tunnel inflows compared to borehole measurements. Stress-permeability coupling in fractured rocks around deep tunnels is strongly dependant on the orientation of the fractures with respect to the tunnel axes (i.e. the increase in effective normal stress acting on the fracture surfaces), and normal and shear stiffness of the fractures. Turbulent flow is expected to occur in many flowing fractures already at relatively moderate rates (e.g. when a fracture with hydraulic aperture of 1mm and 1 m width carries more than 1.5 l/s water, e.g. Wittke 1990).

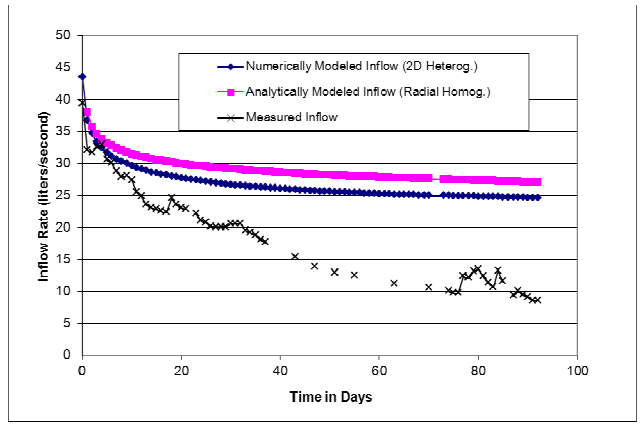

Figure 3.43. Comparison of observed transient inflow, and modeled inflows with analytical equation (radial flow) and 2D numerical hydrodynamic model with free groundwater table and depth-dependant hydraulic properties. Measurements are from fault in Medelser Granite of Gotthard Base Tunnel.

4 SUMMARY AND OUTLOOK

Successful engineering geological predictions for Alpine tunnels require reliable geological models, reliable ground models (with embedded geotechnical parameters of the rock mass) and reliable behavior models. The most critical geological hazards in Alpine tunnels relate to squeezing, spalling/bursting, structurally controlled failures, and water inflows. Brittle tectonic deformation and brittle faults play a key role in the localization and magnitude of these hazards.

4.1 *Geologic Model*

Our capability in the prediction of the geological conditions along tunnel routes has obviously grown in the last centuries, when Alpine tectonics and geology/petrography have been studied in great detail by many European universities and surveys. Today most geological maps at scales of up to 1:25’000 contain reliable geologic and tectonic information. However, most maps do not include brittle faults. The extrapolation of the geological conditions observed at ground surface to depth of 1000 to 2500 m requires fundamental understanding of geological and tectonic processes since Variscan time up to the Holocene. As shown in the previous chapters, our understanding of these processes has reached an impressive level, but nevertheless, even 1000 m wide Permo-Carboniferous troughs or granitic plutons have unexpectedly been encountered in recently excavated Alpine tunnels.

The most important deficits in the predictive power of today’s engineering geological models re-

fer to localized and distributed brittle tectonic faulting. As shown in the example of the Gotthard Base Tunnel, even detailed geological field mapping at the scale of 1:10'000 and the development of comprehensive fault inventories, does not lead to a reliable prediction of faults at tunnel elevation. Especially critical are sub-horizontal faults, which are not detectable on detailed airborne (e.g. LIDAR) based digital terrain models. In addition to the difficulties in the localization, width, architecture and hydromechanical properties of faults cannot be predicted without systematic predrillings from the ongoing excavation.

As shown in many examples, also dispersed or large scale tectonic overprints can have a significant impact on rock mass behavior and especially squeezing. Shear zones with increased tectonic deformation reduce rock mass strength significantly and do not need to follow individual geologic units. Some important Alpine shear zones, like the main thrust separating the Aar and Gotthard Massif, can cross-cut geological units at small, nearly invisible angles.

Several geophysical methods have been proposed in recent years to overcome the restrictions of geological predictions for deep tunnels. Today reliable geophysical mapping of faults in complex tectonic and topographic Alpine settings is only possible at small scales, mainly using single and cross hole radar methods (e.g. Heincke et al. 2005; Spillmann et al. 2007).

4.2 *Ground Model*

Ground models for Alpine tunnels include the description of geotechnical properties of soils (surficial layers and deep incisions) and rocks at various scales. As shown in the case of the Lötschberg Railway and Base Tunnels soils lead to significant hazards even when tunneling through rock at greater depth. The main challenge, however, relates to the characterization of mechanical and hydraulic rock mass properties under the relevant depth and stress conditions. Although not illustrated in the preceding chapters, fracture patterns and fracture properties mapped at ground surface significantly deviate from fracture patterns encountered at the elevation of Alpine tunnels (e.g. Zangerl et al. 2006). Scale effects significantly impact the ground model properties, even in case of intact rock, as shown by axial splitting of lab samples compared to spalling around deep underground excavations. Fluid flow in fractured rocks depend on many factors which are difficult to constrain, and nearly impossible to predict without systematic probing ahead of an advancing tunnel face.

In many projects, variations in hydromechanical properties of rocks and fractures are not carefully evaluated. Extremely large standard deviations are reported, which in fact relate to superficial classifications of rock types and samples tested. Detailed analysis of samples and their test values often lead to a better definition of geotechnically relevant rock types and their property distributions. In future projects spatial variations of rock and rock mass properties should be described more carefully through statistical and geostatistical analyses.

Future progress could also be achieved in the development of ground models through new investigations into the natural formation of fractures in the upper few kilometers of the crust, the factors controlling fracture and fracture network transmissivity in heterogeneous rock, and the strength and deformability of fault rocks in the crystalline basement and sediment cover.

4.3 *Behavior Model*

Behavior models should describe the ground reaction in underground constructions without support measures. Ground reaction is dependent on rock mass type, groundwater, rock stresses, and orientation, size and shape of the opening. As discussed in previous sections many uncertainties remain regarding rock mass properties and groundwater conditions at depth. In addition, large knowledge gaps exist with respect to the stress conditions in Alpine regions. It is known that rock stresses in complex geologic settings like the upper few kilometers of the Alps show large and scale dependent variations. Therefore in most tunnel constructions, stresses are treated as concepts only, without an attempt to reliably measure and analyze rock stresses at depth. It will however be necessary to better constrain the stress magnitudes and variations in these environments, before we can fully understand the observed ground reactions.

This review of engineering geological aspects of deep Alpine tunnels constructed since the 19th century shows that progress depends on experience, technological developments, and - last but not least - our capability to understand our observations. Understanding structurally or stress/strain controlled deformation and failure is a key for future developments in engineering geology as applied to underground excavations. Most geologists are equipped with the necessary descriptive skills to capture the complexity and heterogeneity of geological materials, but they often lack the required understanding of physical processes driving the rock and rock mass response under the complex mechanical and hydraulic conditions around deep underground excavations. Therefore future research in ground engineering has to be interdisciplinary, quantitative, and based on carefully designed field monitoring programs and sophisticated laboratory tests, supported with realistic numerical models capturing

the essential geological components and physical relationships.

ACKNOWLEDGEMENTS

We would like the thank H.J. Ziegler, T. Burri, O. Masset for important contributions to this paper, and the chief engineers (H. Ehrbar) and former project directors (P. Teuscher, P. Zbinden) of the Lötschberg Base Tunnel, Gotthard Base Tunnel and Lyon-Turin Base Tunnel for their support of the research work presented herein.

REFERENCES

Aydan, Ö., Akagi, T., Kawamoto, T. 1993. The squeezing potential of rock around tunnels: theory and prediction. *Rock Mechanics and Rock Engineering*, 2, pp. l37-163.

Barla, G. & Pelizza, S. 2000. TBM tunneling in difficult ground conditions. *GeoEng2000 - An International Conference on Geotechnical and Geological Engineering*, Melbourne: Technomic Publishing Co.

Barla, G. 2001. Tunnelling under squeezing rock conditions. In D.Kolymbas (ed), *Tunnelling mechanics*, Eurosummer School, Innsbruck, Logos Verlag, 169-268.

Barla, G., Bonini, M. and Debernardi, D. 2007. Modelling of tunnels in squeezing rock. *EURO:TUN 2007. 1st Conference on Computational Methods in Tunnelling,* Vienna.

Barla, G., Debernardi, D., and Sterpi D. 2009. Numerical analysis of tunnel response during excavation in squeezing rock by using two constitutive models. *EURO:TUN 2009. 2nd Conference on Computational Methods in Tunnelling,* Bochum.

Barla, G. 2009. Innovative tunnelling construction method to cope with squeeezing at Saint Martin La Porte access adit (Lyon-Torino Base Tunnel). *Rock engineering in difficult conditions in soft rocks and karst. Proc. of Eurock 2009. ISRM Regional Symposium.* Dubrovnik, Croatia

Barton, C.A., Zoback, M.D., Moos, D. 1995. Fluid flow along potentially active faults in crystalline rock. *Geology* 23: 683-686.

Barton, N., Lien, R., Lunde, I. 1974. Engineering classification of rock masses for the design of tunnel supports. *Rock Mechanics,* 6, 4, pp. 189-239.

Bonzanigo, L. & Oppizzi, P. 2006. Low angle fault zones and TBM excavation in Bodio section of Gotthard Base Tunnel. In: Löw S (ed) *Geologie und Geotechnik der Basistunnels am Gotthard und am Lötschberg*. Proc. Symp. Geologie AlpTransit 2005, Zürich: vdf Hochschulverlag AG.

Bosak, P., Ford, D.C., Glazek, J., Horacek, I. 1989. Paleokarst: a systematic and regional review. - p. 725, *Elsevier.*

Branscombe, L., Diederichs, M., Barla, G. 2010. Tunnel liner design in heterogeneous or anisotropic ground. *Rock Mechanics in Civil and Environmental Engineering. Proc. of Eurock 2010. ISRM Regional Symposium,* Lausanne. Switzerland (to be published).

Caine, J.S. & Tomusiak, S.R.A. 2003. Brittle structures and their role in controlling porosity and permeability in a complex Precambrian crystalline-rock aquifer system in the Colorado Rocky Mountain Front Range. *Geol. Soc. of America Bull.* 115: 1410-1424.

Chester, F.M. & Logan, J.M. 1986. Implication for Mechanical Properties of Brittle Faults from tObservations of the Punchbowl Fault Zone, California. *Pure and Applied Geophysics* 124 : 79-106.

Clauser, C. 1992. Permeability of crystalline rocks. *EOS Transactions Amer Geophys U 73(21) :* 233, 237-238.

Clemens, T., Hueckinghaus, D., Sauter, M., Liedl, R., Teutsch, G. 1997. Simulation of the evolution of maze caves. - *In: Proceedings of the 12th International Congress of Speleology; 6th conference on Limestone hydrology and fissured media.* La Chaux-de-Fonds: 65-68.

Coggan, J.S., Pine, R.J, Stead, D., Rance, J.M. 2003. Numerical modelling of brittle rock failure using a combined finite-discrete element approach: implications for rock engineering design. ISRM 2003-S. Afr. Inst. Mining & Metallurgy.

Davis, G.H. & Reynolds, S.J. 1996. Structural geology of rocks and regions. Wiley & Sons, New York

Debernardi, D. 2008. Viscoplastic behaviour and design of tunnels. *PhD Thesis. Doctoral Degree in Geotechnical Engineering. Politecnico di Torino*: 302 pp.

Deer, D.U. 1973. Foliation shear zones – an adverse engineering geologic feature of metamorphic rocks. *J. Boston Soc. Civil Eng.* 60 (4): 163-176

Descoeudres et al. 2005

Diederichs, M.S. 2003. Rock fracture and collapse under low confinement conditions. *Rock Mechanics and Rock Engineering* . Vol. 36 (5) pg 339-381.

Diederichs, M.S. 2007. The 2003 CGS Geocolloquium Address: Damage and spalling prediction criteria for deep tunnelling. *Can. Geotech. J.,* Vol. 44: 9, pp. 1082-1116.

Diederichs, M.S., Kaiser, P.K., Eberhardt, E. 2004. Damage initiation and propagation in hard rock tunnelling and the influence of near-face stress rotation. *Int J Rock Mech & Min Sci.* 41, 785-812.

Diederichs, M.S, Carter, T, Martin C.D. 2010. Practical rock spall prediction in tunnels. *AITES/ITA Conference,* Vancouver. May. 8pgs.

Doe, T. 1991. Fractional dimension analysis of constant-pressure well tests. *SPE paper 22702, Soc. of Petroleum Eng.,* Richardson, Texas.

Davy, P., Bour, O., De Dreuzy, J.R., Darcel, C. 2006. Flow in multiscale fractal fracture networks. In: Cello G, Malamud BD (eds), *Fractal Analysis for Natural Hazards*. Geological Society, London.

El Tani, M. 1999. Water inflow into tunnels. In: Alten T, Backer L, Bollingmo P, Broch E, Holmoy K, Holter KG, Nielsen K (eds), *World Tunnel Congress 1999* on *Challenges for the 21st Century,* Oslo, Norway.

Fairhurst, C. & Cook, N.G.W. 1966. The phenomenon of rock splitting parallel to the direction of maximum compression in the neighbourhood of a surface. *Proc. of the 1st Congress of the Int. Society of Rock Mechanics,* Lisbon, 687-692.

Fellner, D. 1999. Resultate der geologischen Erkundung Sondiersystem Piora. *Vorerkundung und Prognose der Basistunnels am Gotthard und am Lötschberg,* A.A. Balkema, Rotterdam/Brookfield

Frei, B. & Breitenmoser, T. 2006. Geologisch-geotechnische und hydrogeologische Verhältnisse im Vortrieb Amsteg: Vergleich zwischen Prognose und Befund. In: Löw S (ed) *Geologie und Geotechnik der Basistunnels am Gotthard und am Lötschberg*. Proc. Symp. Geologie AlpTransit 2005, Zürich: vdf Hochschulverlag AG.

Fritz, P. 1984. An analytical solution for axisymmetric tunnel problems in elasto-viscoplastic media. *Numerical and analytical methods in geomechanics* 8: 325-342.

Gioda, G. & Cividini, A. 1996. Numerical methods for the analysis of tunnel performance in squeezing rocks. *Rock Mech. Rock Engng.* 29, 171-193.

Goel, P.K., Jethwa, J.L., Paithankar, A.G. 1995. Indian experiences with Q and MR systems. *Tunnelling and Under-*

ground Space Technology 10: 97-109.

Goodman, R.E., Moye, D.G., Schalkwyk, A.V., Javandel, I. 1965. Ground Water Inflows During Tunnel Driving. *Bull Assoc Eng Geol* 2: 39-56.

Harding, H. 1981. Tunnelling history and my own involvement. University of Toronto Press. 258 pp.

Heincke, B., Green, A.G., van der Kruk, J., Horstmeyer, H. 2005. Aquisition and processing strategies for 3D georadar surveying a region characterized by rugged topography. *Geophysics* 71(6): K53-K61.

Herwegh, M. & Pfiffner, O.A. 1999. Die Gesteine der Piora-Zone (Gotthard-Basistunnel). In: Löw, S. & Wyss, R. (eds) *Vorerkundung und Prognose der Basistunnels am Gotthard und am Lötschberg*. Proc. Symp. Geologie AlpTransit 1999, Zürich: A.A. Balkema, Rotterdam/Brookfield

Hoek, E., 2001. Big tunnels in bad rock. Terzaghi Lecture. *ASCE Journal of Geotechnical and Geoenvironmental Engineering, vol. 127, no. 9, September 2001:* 762-740.

Hoek, E. & Marinos, P. 2000. Predicting tunnel squeezing problems in heterogeneous rock masses. *Tunnels and Tunnelling International, Part 1, 32 (11)*: 45-51; *Part 2, 32 (12)*: 33-36.

Hoek, E., Carranza-Torres, C., Corkum, B. 2002. Hoek-Brown failure criterion – 2002 edition. *In Proceedings of NARMS* 2002. Edited by R. Hammah et al.

Hoek, E. & Guevara, R. 2009. Overcoming squeezing in the Yacambú-Quibor Tunnel, Venezuela. *Rock Mech Rock Engng, vol. 42, no. 2*: 389-418.

Ivars, D.M. 2006 Water inflow into excavations in fractured rock – a three-dimensional hydro-mechanical numerical study. *Int J Rock Mech Min Sci* 43: 705-725.

Jacob, C.E. & Lohman, S.W. 1952. Nonsteady flow to a well of constant drawdown in an extensive aquifer. *Trans Amer Geophys Union* 33(4).

Jarsjö, J. & Destouni, G. 2000. Degassing of deep groundwater in fractured rock around boreholes and drifts. *Water Resources Res* 36: 2477-2492.

Kaiser, P.K., McCreath, D., Tannant, D. 1996. Canadian Rockburst Support Handbook. Geomechanics Research Centre and CAMIRO, Sudbury.

Kaiser, P.K., Diederichs, M.S., Martin, D., Sharpe, J., Steiner, W. 2000. Underground Works in Hard Rock Tunnelling and Mining. *In Proceedings of GeoEng2000,* Melbourne, Australia. CDROM.

Kaiser, P.K. 2005. Tunnel stability in highly stressed, brittle ground – rock mechanics considerations for Alpine tunnelling. In: Löw S (ed) *Geologie und Geotechnik der Basistunnels am Gotthard und am Lötschberg*. Proc. Symp. Geologie AlpTransit 2005, Zürich: vdf Hochschulverlag AG.

Kawecki, M.W. 2000. Transient flow to a horizontal water well. *Ground Water* 38(&): 842-850.

Keller, F. & Schneider, T.R. 1982. Der Furka-Basistunnel, Geologie und Geotechnik. *Schweiz. Ingenieur Architekt* 24

Kellerhals, P. & Isler, A. 1998. Lötschberg-Basistunnel: Geologische Voruntersuchungen und Prognose. - Geologische Berichte Nr. 22, Landeshydrologie und -geologie, Bern.

Kovari, K. 1998. Tunnelling in squeezing rock. *Tunnel no. 5*:12-31.

Kovari, K. & Fechtig, R. 2000. Historical Tunnels in the Swiss Alps. Stäubli AG, Zürich.

Kovari, K. 2005. Method and device for stabilizing a cavity excavated in underground construction. US Patent Appl. 20050191138, 2005.

Laws, S., Eberhardt, E., Loew, S., Descoeudres, F. 2003. Geomechanical Properties of Shear Zones in the Eastern Aar Massif, Switzerland and their Implication on Tunnelling. *Rock Mechanics and Rock Engineering,* 36 (4): 271-303.

Lei, S. 1999. An Analytical Solution for Steady Flow into a Tunnel. *Ground Water* 37: 23-26.

Lei, S. 2000. Steady Flow into a Tunnel with a Constant Pressure Head. *Ground Water* 38: 643-644.

Loew, S. 2002. Groundwater Hydraulics and Environmental Impacts of Tunnels in Crystalline Rocks. Van Rooy, J. L., & Jermy C.A. (eds), *Engineering Geology for Developing Countries*, Proc. 9th Congress IAEG, Durban.

Loew, S., Ziegler, H.-J., Keller, F. 2000. Alptransit: Engineering Geology of the Longest Tunnel System. *GeoEng2000 - An International Conference on Geotechnical and Geological Engineering*, Melbourne: Technomic Publishing Co.

Loew, S., Luetzenkirchen, V., Ofterdinger, U., Zangerl, C., Eberhardt, E., Evans, K. 2007. Environmental impacts of tunnels in fractured crystalline rocks of the Central Alps. In: Krasny, J. & Sharp, J.M. (eds), *Groundwater in Fractured Rocks*, London: Taylor and Francis, IAH Selected Papers on Hydrogeology 9: 507-526.

Lombardi, G. & Amberg, W. 2005. Untersuchungen zur Ermittlung der Empfindlichkeit der Staumauer Ferden. *Wasser, Energie, Luft* 11/12: 294-296.

Long, J.C.S., Karasaki, K., Davey, A., Peterson, J., Landsfeld, M., Kemeny, J., Martel, S. 1991. An Inverse Approach to the Construction of Fracture Hydrology Models Conditioned by Geophysical Data An Example from the Validation Exercises at the Stripa Mine. *Int J Rock Mech Min Sci & Geomech Abstr* 28: 121-142

Lützenkirchen, V.H. 2002. Structural Geology and Hydrogeology of Brittle Fault Zones in the Central and Eastern Gotthard Massif, Switzerland. PhD Thesis, ETH, Zürich, Switzerland

Maidl, B. & Handke, D. 1993. Overcoming a collapse in the Karawanken tunnel. - *Tunnels and Tunnelling*. 25(6): 30-32

Marinos, P. 2005. Experiences in tunneling through karstic rocks. In: *Water resources & environmental problems in Karst, KARST 2005*. Proc. IAH International Conference, Belgrade: 617-644

Martin, C.D. 1997. 17th Canadian Geotech. Colloq: The effect of cohesion loss and stress path on brittle rock strength. *Can. Geotech. Journal,* 34 (5), 698-725.

Masset, O. & Loew, S. 2010. Hydraulic conductivity distribution in crystalline rocks, derived from inflows to tunnels and galleries in the Central Alps, Switzerland. *Hydrogeol J* published online. DOI: 10.1007/s10040-009-0569-1

Maurer, H.R., Löw, S., Lützenkirchen, V., Green, A. 2000. Geophysikalische Vorauserkundung von Karststrukturen in der Doldenhorn-Decke. Unpublished report AlpTransit, Lötschberg-Basistunnel

Moon, J. & Fernandez, G. 2010. Effect of excavation-induced groundwater level drawdown on tunnel inflow in a jointed rock mass. *Eng Geol* 110: 33-42

Moreno, L. & Neretnieks, I. 1993. Flow and nuclide transport in fractured media: The importance of the flow-wetted surface for radionuclide migration. *J Contaminant Hydrol* 13: 49-71.

Oberti, G., Goffi, L., Luciani, L. 1969. Misure di coazione nelle rocce in corrispondenza di gallerie. *1st International Congrees on Technical Problems in the Construction of Tunnels.* 425-434.

Ottiger, R. 2006. Hydrogeologie Vortrieb Ferden. In: Löw S (ed) *Geologie und Geotechnik der Basistunnels am Gotthard und am Lötschberg*. Proc. Symp. Geologie AlpTransit 2005, Zürich: vdf Hochschulverlag AG: 167-179.

Palmer, A. 1991. Origin and morphology of limestone caves. *Geol. Soc. of America Bull*. Vol. 103: 1-21

Panet, M. 1996. Two case histories of tunnels through squeezing rocks. *Rock Mechanics and Rock Engineering*, 29 (3), pp. 155-164

Passchier, C.W. & Trouw, R.A.J. 1996. Microtectonics. Springer, Berlin Heidelberg New York

Pelli, F., Kaiser, P.K., Morgenstern, N.R. 1991. An interpretation of ground movements recorded during construction of the Donkin-Morien tunnel. *Can. Geotech. Journal,* 28 (2), 239-254.

Pesendorfer, M. & Loew, S. 2007. Detection efficiency of long horizontal predrillings to identify water conductive structures. *Felsbau* 25(4): 18-27

Pesendorfer, M. & Loew, S. 2009. Subsurface exploration and transient pressure testing from a deep tunnel in fractured and karstified limestones (Lötschberg Base Tunnel, Switzerland). *Int J Rock Mech Min Sci* 47: 121-137

Pesendorfer, M., Loew, S., Zappa, M. 2010. Environmental impacts of the Lötschberg Base and Crest Tunnels, Switzerland. In: Vrkljan (ed.), *Rock Engineering in Difficult Ground Conditions – Soft Rocks and Karst*; Proc. Intern. Symp. Eurock. London: Taylor and Francis Group.

Ramsay, J.G. & Huber, M. 1987. *The techniques of modern structural geology*, Vol. II. Academic Press, London

Raymer, J.H. 2001a. Groundwater Inflow into Hard-Rock Tunnels. *Tunnels and Tunneling International*, Polygon Media Ltd, London, 50-53

Raymer, J.H. 2001b. Predicting Groundwater Inflow into Hard-Rock Tunnels: Estimating the High-End of the Permeability Distribution. In: Hansmire, W.H. and Gowring, I.M. (eds.), *Proceedings of the Rapid Excavation and Tunneling Conference,* Society of Mining, Metallurgy and Exploration.

Röthlisberger, B. 2006. Geologisch-geotechnische Erkundungen und Überwachung in der Multifunktionsstelle Faido. In: Löw S (ed) *Geologie und Geotechnik der Basistunnels am Gotthard und am Lötschberg*. Proc. Symp. Geologie AlpTransit 2005, Zürich: vdf Hochschulverlag AG.

Sandrone, F., Dudt, J.P., Labiouse, V., Descoudres, F., 2006. Analysis of delayed convergences in a carbone zone of the Lötschberg tunnel. Multiphysics Coupling and Long Term Behaviour in Rock Mechanics. *Proc. of Eurock 2006. ISRM Regional Symposium,* Liege, Belgium: 351- 356

Schneider, T.R. 1999. Gotthard-Basistunnel: Strategie der geologischen Untersuchungen. In: Löw, S. & Wyss, R. (eds) *Vorerkundung und Prognose der Basistunnels am Gotthard und am Lötschberg*. Proc. Symp. Geologie AlpTransit 1999, Zürich: A.A. Balkema, Rotterdam/Brookfield

Schubert, P. & Morinko, T. 1989. Vortrieb des Karawankentunnels im tektonisch stark beanspruchten Südabschnitt. - *Felsbau* 7(2): 67-68

Schubert, W. 1993. Erfahrungen bei der Durchörterung von Störzonen bei Österreichischen Tunneln. *Felsbau*, 11: 287-290

Schubert, W. 1996. Dealing with squeezing conditions in alpine tunnels. *Rock Mech Rock Engng, vol. 29, no. 3*: 145-153

Schubert, W. 2006. Tunneling in fault zones – the importance of on-site engineering. In: Löw S (ed) *Geologie und Geotechnik der Basistunnels am Gotthard und am Lötschberg*. Proc. Symp. Geologie AlpTransit 2005, Zürich: vdf Hochschulverlag AG.

Schubert, W. & Riedmüller, G. 1997. Influence of faults on tunnelling. *Felsbau* 15: 483-488

Schubert, W., Moritz, D., Sellner, P., Blümel, M. 1999. Tunnelling in squeezing ground recent improvements. *Felsbau 17 (1)*: 56-58

Sibson, R.H. 1977. Fault rocks and fault mechanisms. *J. Geol. Soc.* London, 133: 191-213

Singh, B., Jethwa, J.L., Dube, A.K., Singh, B. 1992. Correlation between observed support pressure and rock mass quality. *Tunnelling and Underground Space Technology*, 7, pp. 59-74.

Snow, D.T. 1969. Anisotropic Permeability of Fractured Media. *Water Resources Res* 5: 1273-1289.

Spillmann, T., Maurer, H., Willenberg, H., Evans, K.F., Heincke. B., Green, A.G. 2007. Characterization of an unstable rock mass based on borehole logs and diverse borehole radar data. *Journal of Applied Geophysics*, 61(1), 16-38

Stacey, T.R., & De Jongh, C.L. 1977. Stress fracturing around a deep level bored tunnel. *Journal South African Institute of Mining and Metallurgy,* 78: 124-133.

Sterpi, D. & Gioda, G. 2009. Visco-plastic behaviour around advancing tunnels in squeezing rock. *Rock Mech. Rock Engng.*, 42, 319-339

Stini, J. 1950. Tunnelbaugeologie, Springer-Verlag, Wien

Stober, I. 1995. Die Wasserführung des kristallinen Grundgebirges. Enke-Verlag, Stuttgart

Stober, I. 1997. Permeabilities and Chemical Properties of Water in Crystalline Rocks of the Black Forest, Germany. *Aquatic Geochemistry* 3: 43-60

Stober, I. & Bucher, K. 2007. Hydraulic properties of the crystalline basement. *Hydrogeol J* 15: 213-224

Strickler, A. 1923. Beiträge zur Frage der Geschwindigkeitsformel und der Rauhigkeitszahlen für Ströme, Kanäle und geschlossene Leitungen. - Mitt. Amt. f. Wasserwirtschaft Berlin, Nr. 16.

Tannant, D.D. & Wang, C. 2004. Thin tunnel liners modelled with Particle Flow Code. *Engineering Computations: Int. J. Comp-Aided Eng,* 21(2-4): 318-342.

Thérond, R. 1973. Recherche sur l'étanchéité des lacs de barrage en pays karstique. Monograph, „Eyrolles", Paris, pp. 444.

Vuilleumier, F. & Seingre, G. 2002. Les Tassements de St. German. In: FGU Fachgruppe für Untertagebau (ed), *AlpTransit Tagung 2002*, Proc. Fachtagung für Untertagebau Interlaken, Zürich: Dokumentation SIA D 0177: 95-100.

Vuilleumier, F. & Aeschbach, M. 2004. The Lötschberg base tunnel – lessons learned from the construction of the tunnel. Presentation at 1º Congresso Brasileiro de Túneis e Estruturas Subterrâneas, Seminário Internacional South American Tunnelling.

Vyazmensky, A., Elmo, D., Stead, D., Rance, J. 2007. Combined finite-discrete element modelling of surface subsidence associated with block caving mining *Proceedings of 1st Canada-U.S. Rock Mech. Symp.* Vancouver: 467-475.

Wallace, R.E., & Morris, H.T. 1986. Characteristics of Faults and Shear Zones in Deep *Mines. Pure and Applied Geophysics* 124: 107-125

Wittke, W. 1990. Rock Mechanics, Springer-Verlag, Wien

Zangerl, C., Eberhardt, E., Evans, K.F., Loew, S. 2008a. Consolidation settlements above deep tunnels in fractured crystalline rock: Part 1 - Investigations above the Gotthard highway tunnel, *Int J Rock Mech Min Sci* 45: 1195-1210

Zangerl, C., Evans, K.F., Eberhardt, E., Loew, S. 2008b. Consolidation settlements above deep tunnels in fractured crystalline rock: Part 2 – Numerical analysis of the Gotthard highway tunnel case study. *Int J Rock Mech Min Sci* 45: 1211-1225

Zhang, L. & Franklin, J.A. 1993. Prediction of water flow into rock tunnels: an analytical solution assuming a hydraulic conductivity gradient. *Int J Rock Mech Min Sci* 30: 37-46

Zhao, J. 1998. Rock mass hydraulic conductivity of the Bukit Timah granite, Singapore. *Eng Geol* 50: 211-216

Ziegler, H.-J. 2004. Vergleich Prognose/Befund und Erkenntnisse. In: FGU Fachgruppe für Untertagebau (ed), *AlpTransit Tagung 2004*, Proc. Fachtagung für Untertagebau Interlaken, Zürich: Dokumentation SIA D 0202: 55-58

Ziegler, H.-J. 2006. Geologisches Befundprofil Lötschberg-Basistunnel 1:50'000. In: Löw S (ed) *Geologie und Geotechnik der Basistunnels am Gotthard und am Lötschberg*.

Proc. Symp. Geologie AlpTransit 2005, Zürich: vdf Hochschulverlag AG.